

AD-A261 884



1

WL-TR-92-4017



X-RAY COMPUTED TOMOGRAPHY FOR FAILURE ANALYSIS

Richard H. Bossi
Alan R. Crews
Gary E. Georgeson

Boeing Defense & Space Group
P.O. Box 3999
Seattle, WA 98124



August 1992

Interim Report for Period May 1991 to January 1992

Approved for public release; distribution is unlimited

MATERIALS DIRECTORATE
WRIGHT LABORATORY
AIR FORCE SYSTEMS COMMAND
WRIGHT-PATTERSON AIR FORCE BASE, OHIO 45433-6533

93-05133



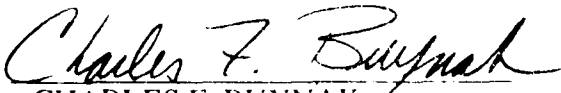
5628

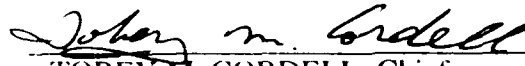
NOTICE

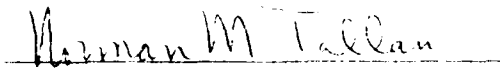
When Government drawings, specifications, or other data are used for any other purpose other than in connection with a definitely Government-related procurement, the United States Government incurs no responsibility or any obligation whatsoever. The fact that the government may have formulated or in any way supplied the said drawings, specifications, or other data, is not to be regarded by implication, or otherwise in any manner construed, as licensing the holder, or any other person or corporation; or as conveying any rights or permission to manufacture, use, or sell any patented invention that may be related thereto.

This report is releasable to the National Technical Information Service (NTIS). At NTIS, it will be available to the general public, including foreign nations.

This technical report has been reviewed and is approved for publication.


CHARLES F. BUYNAK
Nondestructive Evaluation Branch
Metals and Ceramics Division


TOBEY M. CORDELL, Chief
Nondestructive Evaluation Branch
Metals and Ceramics Division


NORMAN N. TALLAN, Chief
Metals and Ceramics Division
Materials Directorate

If your address has changed, if you wish to be removed from our mailing list, or if the addressee is no longer employed by your organization please notify WL/MLLP, WPAFB, OH 45433-7817 to help us maintain a current mailing list.

Copies of this report should not be returned unless return is required by security considerations, contractual obligations, or notice on a specific document.

REPORT DOCUMENTATION PAGE			Form Approved OMB No. 0704-0188	
1. AGENCY USE ONLY (Leave Blank)		2. REPORT DATE August 31, 1992	3. REPORT TYPE AND DATES COVERED Interim May 1991 - Jan 1992	
4. TITLE AND SUBTITLE X-Ray Computed Tomography for Failure Analysis			5. FUNDING NUMBERS F33615-88-C-5404 PE: 63112F PR: 3153 TA: 00 WU: 06	
6. AUTHOR(S) Richard H. Bossi, Alan R. Crews and Gary E. Georgeson				
7. PERFORMING ORGANIZATION NAME(S) AND ADDRESS(ES) Boeing Defense & Space Group P.O. Box 3999 Seattle, WA 98124-2499			8. PERFORMING ORGANIZATION REPORT NUMBER	
9. SPONSORING/MONITORING AGENCY NAME(S) AND ADDRESS(ES) Charles Buynak (513) 255-9802 Wright Laboratory, Materials Directorate WL/MLLP Wright-Patterson AFB, OH 54533-6533			10. SPONSORING/MONITORING AGENCY REPORT NUMBER WL-TR-91-4102	
16. SUPPLEMENTARY NOTES				
12a. DISTRIBUTION/AVAILABILITY STATEMENT Approved for public release; distribution is unlimited			12b. DISTRIBUTION CODE	
13. ABSTRACT (Maximum 200 words) Under a preliminary testing task assignment of the Advanced Development of X-Ray Computed Tomography Application program, computed tomography (CT) has been studied for its potential as a tool to assist in failure analysis investigations. CT provides three-dimensional spatial distribution of material that can be used to assess internal configurations and material conditions nondestructively. This capability has been used in failure analysis studies to determine the position of internal components and their operation. CT is particularly advantageous on complex systems, composite failure studies, and testing under operational or environmental conditions. CT plays an important role in reducing the time and effort of a failure analysis investigation. Aircraft manufacturing or logistical facilities perform failure analysis operations routinely and could be expected to reduce schedules, reduce costs and/or improve evaluation on about 10 to 30 percent of the problems they investigate by using CT.				
14. SUBJECT TERMS Computed Tomography (CT), Failure Analysis, Electromechanical System, Materials, Cost/Benefit, Electronic, Honeycomb, Solenoid, Hydraulic, Nondestructive Evaluation (NDE)			15. NUMBER OF PAGES 55	
			16. PRICE CODE	
17. SECURITY CLASSIFICATION OF REPORT Unclassified	18. SECURITY CLASSIFICATION OF THIS PAGE Unclassified	19. SECURITY CLASSIFICATION OF ABSTRACT Unclassified	20. LIMITATION OF ABSTRACT UL	

TABLE OF CONTENTS

Section	Page
1.0 INTRODUCTION	1
1.1 Computed Tomography	1
1.2 Scope and Objective	1
2.0 TEST PLAN	3
2.1 Part Acquisition	3
2.2 CT Testing	3
2.3 Data Evaluation	3
3.0 ELECTROMECHANICAL SYSTEMS	4
3.1 Autobrake Module, Type 1	4
3.2 Autobrake Module, Type 2	8
3.3 Solenoid Valve	12
4.0 ELECTRICAL COMPONENTS	18
4.1 Instrumentation Wafer Antenna	18
4.2 Raceway Potted Cable Assembly	20
5.0 MECHANICAL	22
5.1 Drag Brace with Experimental Bearing	22
5.2 Fuel Line	26
6.0 MATERIALS	29
6.1 Failure Analysis of Honeycomb Panel	29
6.2 Composite Damage Analysis	35
7.0 COST BENEFIT ANALYSIS	38
7.1 Failure Analysis Laboratory Application	38
7.2 Cost Savings Examples	41
7.2-1 Autobrake Modules	41
7.2-2 Instrumentation Wafer Antenna	41
7.2-3 Raceway Potted Cable Assembly	42
7.3 CT System Procurement	42
8.0 CONCLUSIONS AND RECOMMENDATIONS	43
8.1 Conclusions	43
8.2 Recommendations	44
9.0 REFERENCES	45
APPENDIX - RADIOGRAPHIC TECHNIQUES	46
A1 Film Radiography	46
A2 Digital Radiography	47
A3 Computed Tomography	48
A3.1 Conventional CT	48
A3.2 Cone Beam CT	49

Accession For	
NTIS CRA&I	<input checked="" type="checkbox"/>
DTIC TAB	<input type="checkbox"/>
Unannounced	<input type="checkbox"/>
Justification	
By _____	
Distribution /	
Availability Codes	
Dist	Avail and/or Special
A-1	

LIST OF FIGURES

Figure		Page
3.1-1	Pictorial drawing of the autobrake module, Type 1.	4
3.1-2	Schematic of the autobrake module mechanism.	6
3.1-3	Breakout drawing of the autobrake control module. Item #12 is the feedback spring.	6
3.1-4	CT slice through the autobrake module at the height of the pressure control servovalve.	7
3.1-5	Enlargement of the feedback spring showing mislocation.	7
3.2-1	Pictorial drawing of the autobrake module, Type 2.	8
3.2-2	Schematic drawing of the autobrake module, Type 2.	9
3.2-3	Breakout drawing of the autobrake module shutoff valve assembly.	10
3.2-4	CT slice through the autobrake module at the height of the pressure control servovalve.	11
3.2-5	Enlargement of the shutoff spool valve showing gap.	11
3.3-1	Pictorial drawing of the solenoid valve assembly.	13
3.3-2	Cutaway drawing of the solenoid valve.	13
3.3-3	Longitudinal CT slice through the burned solenoid valve.	14
3.3-4	Longitudinal CT slice through a new solenoid valve.	14
3.3-5	CT slice through the new (left) and burned (right) solenoid valves at CT system height 488.5.	15
3.3-6	CT slice through the new (left) and burned (right) solenoid valves at CT system height 488.0	16
3.3-7	CT slice through the burned (left) and new (right) solenoid valves at CT system height 487.5.	15
3.3-8	CT slice through the new (left) and burned (right) solenoid valves at CT system height 487.5.	16
3.3-9	CT slice through the new (left) and burned (right) solenoid valves at CT system height 486.5.	16
3.3-10	CT slice through the new (left) and burned (right) solenoid valves at CT system height 486.0.	16
3.3-11	CT slice through the new (left) and burned (right) solenoid valves at CT system height 485.5.	17
3.3-12	CT slice through the new (left) and burned (right) solenoid valves at CT system height 485.0.	17
4.1-1	Photograph of an instrumentation wafer antenna.	18
4.1-2	CT slice through the instrumentation wafer antenna.	19
4.1-3	CT slice through the instrumentation wafer antenna.	19
4.2-1	CT slice through the raceway cable in a region of surface discoloration for a failed cable.	20
4.2-2	CT slice through the raceway cable near the termination of the cable at the connector.	21
5.1-1	Drawing of the drag brace.	22
5.1-2	Schematic drawing showing the location of CT slices 1, 2, 3 and 4 on the drag brace bushing.	23

5.1-3	Cross-section drawing of drag brace elastomeric bushing assembly with 0 and 90 degree cuts through Figure 5.1-2.	24
5.1-4	CT slice at location 1 on the drag brace bushing.	25
5.1-5	CT slice at location 2 on the drag brace bushing.	25
5.1-6	CT slice at location 3 on the drag brace bushing.	25
5.1-7	CT slice at location 4 on the drag brace bushing.	25
5.2-1	CT slice of a fuel line under vacuum conditions (2X actual size) showing teflon inner tube and braided stainless steel outer tube.	26
5.2-2	CT slice of the fuel line under ambient pressure.	27
5.2-3	CT slice of the fuel line at operational pressure.	28
6.1-1	Photograph of a graphite/epoxy honeycomb panel with a Ti alloy core.	30
6.1-2	Sketch of the panel showing CT slice locations.	30
6.1-3	CT slice at location A.	31
6.1-4	CT slice at location A with gray scale in image adjusted to observe the honeycomb.	31
6.1-5	CT slice at location B.	32
6.1-6	2x enlargement of CT image at location B.	32
6.1-7	CT slice at location D.	32
6.1-8	Left half of the CT slice at location C.	33
6.1-9	Schematic of suggested selective loading of honeycomb panel.	33
6.1-10	Schematic of the frame constraints for loading of the test sample.	34
6.2-1	Photograph of the graphite epoxy composite sample a) impacted test panel, b) small coupon removed from the damaged region.	35
6.2-2	CT slice through the center of the impacted coupon showing delaminations.	35
6.2-3	CT slice through a damaged graphite epoxy sample showing a transverse crack and a 0 degree crack intersecting a fastener hole.	36
6.2-4	Three-dimensional model of the damaged region around a fastener hole constructed from high resolution CT data.	37
7.1-1	Approximate performance range for the CT systems of Table 7.1-3.	40
7.1-2	Bargraph showing the relative percentage of the workload applicable to each CT system type for the failure analysis laboratories.	41
7.3-1	Laboratory size for microfocus CT system acquisition for various percentages of CT applicability to product evaluation.	42
A1-1	Film radiography.	46
A2-1	Digital radiography.	47
A3-1	Computed tomography.	48
A3-2	Cone beam CT.	49

LIST OF TABLES

Table	Page
7.1-1	Workload for Parts Engineering Failure Analysis Lab. 38
7.1-2	Workload for Equipment Quality Analysis Lab. 38
7.1-3	Categories of CT Systems 40

SUMMARY

Under a preliminary testing task assignment of the Advanced Development of X-ray Computed Tomography Application program, computed tomography (CT) has been studied for its potential as a tool to assist in failure analysis investigations. CT provides three-dimensional spatial distribution of material that can be used to assess internal configurations and material conditions nondestructively. This capability has been used in failure analysis studies to determine the position of internal components and their operation. CT is particularly advantageous on complex systems, composite failure studies, and testing under operational or environmental conditions. CT plays an important role in reducing the time and effort of a failure analysis investigation. Aircraft manufacturing or logistical facilities perform failure analysis operations routinely and could be expected to reduce schedules, reduce costs and/or improve evaluation on about 10 to 30 percent of the problems they investigate by using CT.

ACKNOWLEDGEMENTS

The authors extend special thanks to the Boeing Parts Failure Analysis Laboratory and the Boeing Equipment Quality Analysis Laboratories for their assistance.

DISCLAIMER

The information contained in this document is neither an endorsement nor criticism for any X-ray imaging instrumentation or equipment used in this study.

1.0 INTRODUCTION

The goal of the Advanced Development of X-Ray Computed Tomography Applications demonstration (CTAD) program is to evaluate inspection applications for which X-ray computed tomography (CT) can provide a cost-effective means to evaluate aircraft/aerospace components. The program is "task assigned" so that specific CT applications or application areas can be addressed in separate projects. Three categories of task assignments are employed in the program: 1) preliminary tests where a variety of parts and components in an application area are evaluated for their suitability to CT examinations, 2) final tests, where one or a few components are selected for detailed testing of CT capability to detect and quantify defects, and 3) demonstrations, where the economic viability of CT to the inspection problem are analyzed and the results presented to government and industry. This interim report is the result of a final task assignment study on failure analysis. Additional task assignment reports issued by the CTAD program are listed in References 1 through 9.

1.1 Computed Tomography

X-ray computed tomography (CT) is a powerful nondestructive evaluation technique that was conceived in the early 1960's and has been developing rapidly ever since. CT uses measurements of X-ray transmission from many angles about a component to compute the relative X-ray linear attenuation coefficient of small volume elements and presents them as a cross-sectional image map. The clear images of an interior plane of an object are achieved without the confusion of superposition of features often found with conventional film radiography. CT can provide quantitative information about the density/constituents and dimensions of the features imaged. The Appendix compares the basic radiographic (RT), digital radiography (DR), and CT techniques utilized in the CTAD program.

Although CT has been predominantly applied to medical diagnosis, industrial applications have been growing over the past decade. Medical systems are designed for high throughput and low dosages specifically for humans and human sized objects. These systems can be applied to industrial objects that have low atomic number and are less than one-half meter in diameter. Industrial CT systems do not have dosage and size constraints. They are built in a wide range of sizes from the inspection of small components (such as test coupons or jet engine turbine blades) using low to mid-energy (hundreds of kV) X-ray sources to the inspection of large ICBM missiles requiring high (MV level) X-ray energies. The appropriate industrial CT system required for any particular component inspection depends on the size of the component and sensitivity required to evaluate the details of interest in the component.

1.2 Scope and Objective

This task assignment, designated "Task 11 - Failure Analysis," was a final testing task directed at the evaluation of CT as a tool, useful in failure analysis studies.

The overall goal of this task assignment was the evaluation of the technical feasibility and economic viability of using CT as part of a failure analysis organization. Specific objectives included the determination of CT system requirements for typical internal component evaluation in aircraft equipment evaluation, and the necessary sensitivity of CT to be useful in a variety of failure analysis studies, such as assembly verification, dimensional tolerances, foreign object detection, defects, and material variations.

An additional goal for the task assignment is to evaluate the type of activity a failure analysis laboratory performs and assess how CT could assist in those investigations. The assessment includes whether or not CT is of economic viability and if so, in what capacity.

2.0 TEST PLAN

The test plan for the failure analysis task involved the cooperation of aircraft failure analysis laboratories to provide records of the typical workload, acquisition of test components that CT might assist in the investigation, CT scanning, evaluation of the effectiveness of CT and its economic benefit, development of demonstration plans and reporting.

2.1 Part Acquisition

The primary sources of test items for this task assignment were the Boeing Commercial Airplane Group Renton and Everett Equipment Quality Analysis laboratories and the Boeing Defense & Space Group Parts Analysis Laboratory. These organizations provided lists of the type of components that they investigate and provided test samples where CT appeared to offer advantages over other techniques. The primary categories of the failure analysis items were electromechanical systems and electronic systems. Additional samples for failure analysis were sought from engineering organizations and the Air Force in the areas of mechanical parts and materials.

2.2 CT Testing

CT testing at appropriate facilities was based on results from previous studies with respect to the system capability to handle the part sizes, material densities, and resolutions. In some cases alternative methods, such as radiography and radioscopy, to evaluate the failure analysis study were performed and are noted.

2.3 Data Evaluation

Data evaluation of the failure analysis investigation primarily consisted of the assessment of the detectability of various features from the CT images. In some cases, destructive test information was later available for comparison. The economic factors in choosing to use CT or alternative approaches to reach conclusions for the failure analysis were assessed and reported.

3.0 ELECTROMECHANICAL SYSTEMS

Electromechanical systems are complex in nature not only from their physical construction but also from the functional aspects and the environmental extremes that they must withstand. They are typically an interface between two systems or responsible for control of another system. This control can be with or without feedback. When feedback mechanisms are involved, the electromechanical devices are more complicated internally, and it is more difficult to interpret malfunctions from simple external measurements.

The two criteria for classifying a device as electromechanical are electrical input or output, and mechanical motion. The mechanical motion that occurs will be either translational or rotational, and can be either an input, output or intermediate process. This mechanical motion typically controls a hydraulic/pneumatic source/supply or provides mechanical restraint or motion.

3.1 Autobrake Module, Type 1

Autobrake modules are precision integrated hydraulic control units which provide controlled pressure to an aircraft autobrake system; this in conjunction with the aircraft flight control electronics provides skid control, tailored deceleration profile, and selectable braking distance. Figures 3.1-1 is a pictorial drawing of one type of module, labeled Type 1, which is approximately 150 mm (6 in) on a side.

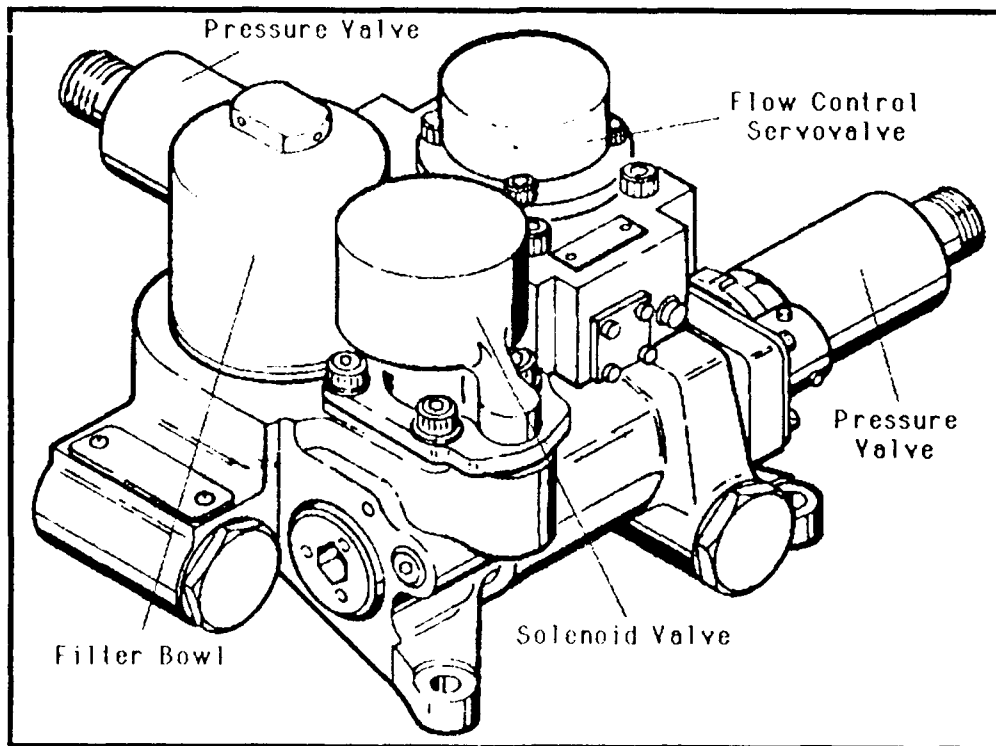


Figure 3.1-1 Pictorial drawing of the autobrake module, Type 1.

The control is accomplished by applying supply pressure through a filter to the shutoff and solenoid valves, see Figure 3.1-2. The shutoff valve is controlled by the solenoid valve. With the solenoid valve in the deenergized position, supply pressure is continuously applied to the small end of the unequal area piston of the shutoff valve and the large end is vented to the return port. In this condition, the fluid supply to the servovalve and pressure switches is shut off. With the solenoid valve energized, supply pressure is applied to both the small and large ends of the unequal area piston causing the piston to be displaced and the supply port to be connected to the control valve and the first stage. The first stage provides a control pressure which acts on one end of the control valve spool. The brake pressure acts on the opposite end of the control valve spool through a 40% area piston. The control valve provides the load flow required to maintain the load pressure at a fixed ratio of 2.56 times the first stage control pressure. The spool controls the output pressure.

An autobrake unit, that was experiencing out-of-specification hydraulic pressure response, was evaluated radiographically, but the images contained a confusion of features with very poor sensitivity to internal detail. Digital radiography (DR) was also performed on the unit and compared to the film radiograph the DR was clearly superior for this analysis. However projection radiography of a complex component is not sufficient and in fact showed convincingly that CT or disassembly would be required to determine the failure mechanism of this assembly.

Computed tomography evaluation of the autobrake control module was performed on a medium resolution (~1 line-pair/mm) system. CT slice heights were selected to inspect the suspect pressure control servovalve and other regions of interest such as orifices, valves and moving parts. Figure 3.1-3 shows a breakout drawing of the module. The first CT slice, was taken to inspect the feedback spring, no. 12, in Figure 3.1-3, that seats in detent holes on items no. 8 and no. 17. The CT image shown in Figure 3.1-4, with an enlargement of the spring shown in Figure 3.1-5, clearly indicate that the feedback spring of the pressure control servovalve had jumped out of the detents. This was the cause of the out-of-specification hydraulic pressure response. When the spring is not properly centered in the hole, this leads to rubbing, binding, and scratching as observed in past failure analysis investigations of this unit. Subsequent CT slices, not shown here, demonstrated the capability to adequately evaluate the other areas of interest in the assembly.

CT specifically provided the analyst direct evidence the spring was clearly not in the detent. This cannot be determined with certainty from any other nondestructive technique. Because disassembly causes the spring to float free when the end of the servovalve portion of the unit is removed, even disassembly of the unit would force the analyst to rely on the indirect evidence of scratches and rub marks.

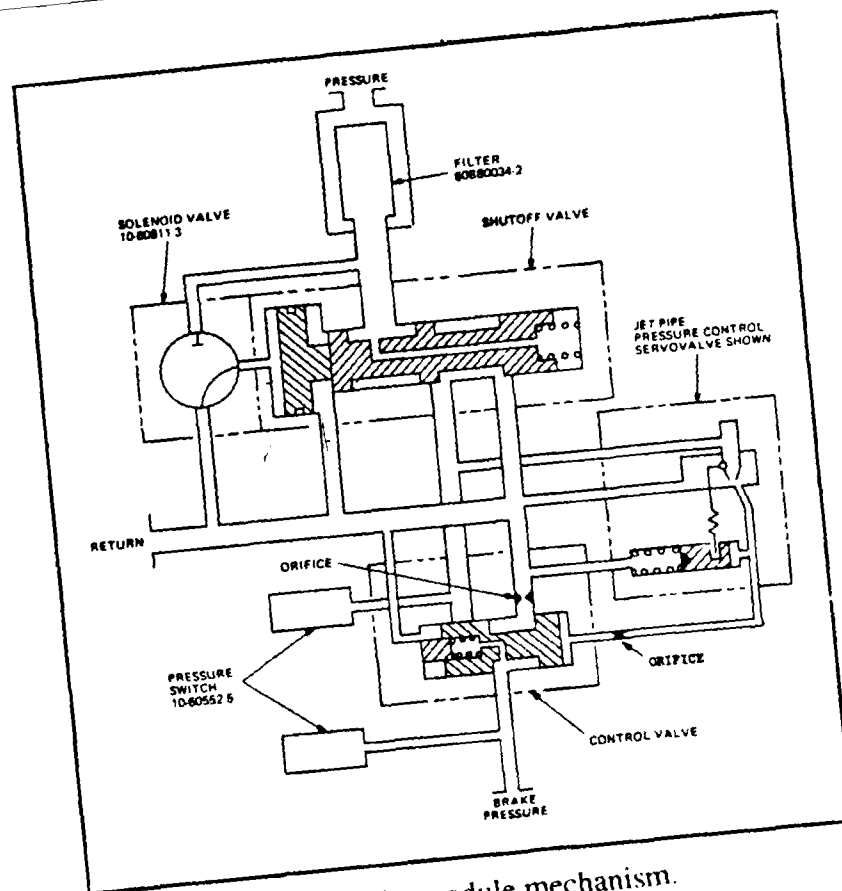


Figure 3.1-2 Schematic of the autobrake module mechanism.

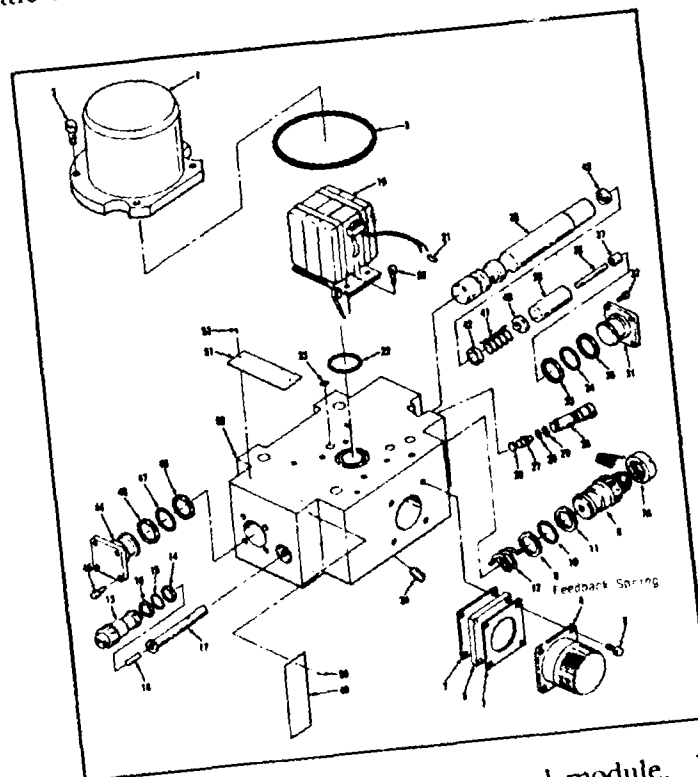


Figure 3.1-3 Breakout drawing of the autobrake control module. Item #12 is the feedback spring.

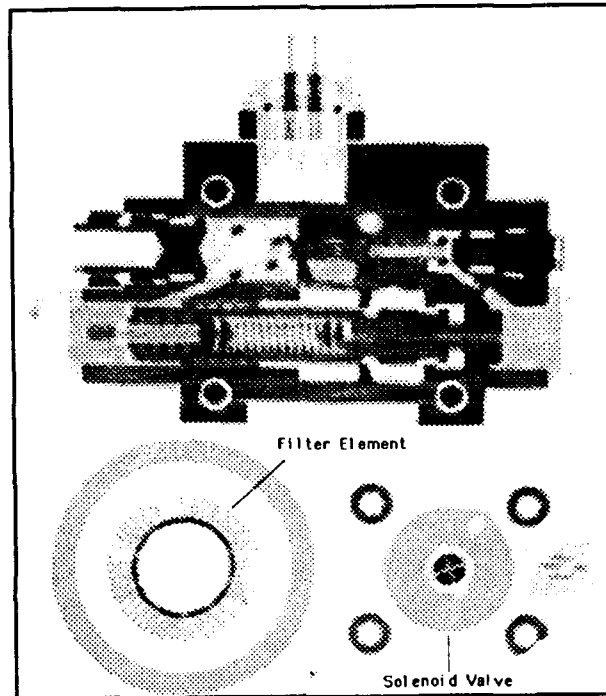


Figure 3.1-4 CT slice through the autobrake module at the height of the pressure control servovalve.

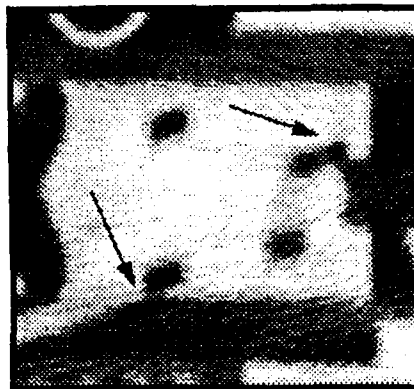


Figure 3.1-5 Enlargement of the feedback spring showing mislocation.

3.2 Autobrake Module, Type 2

A second type of autobrake valve module, shown pictorially in Figure 3.2-1, provides amplitude modulation of hydraulic source pressure to the anti-skid system using a two stage electrohydraulic pressure control servo valve. Figure 3.2-2 shows a schematic of this module. The module also contains a three-way solenoid valve, a piston-driven shutoff valve and two pressure switch assemblies.

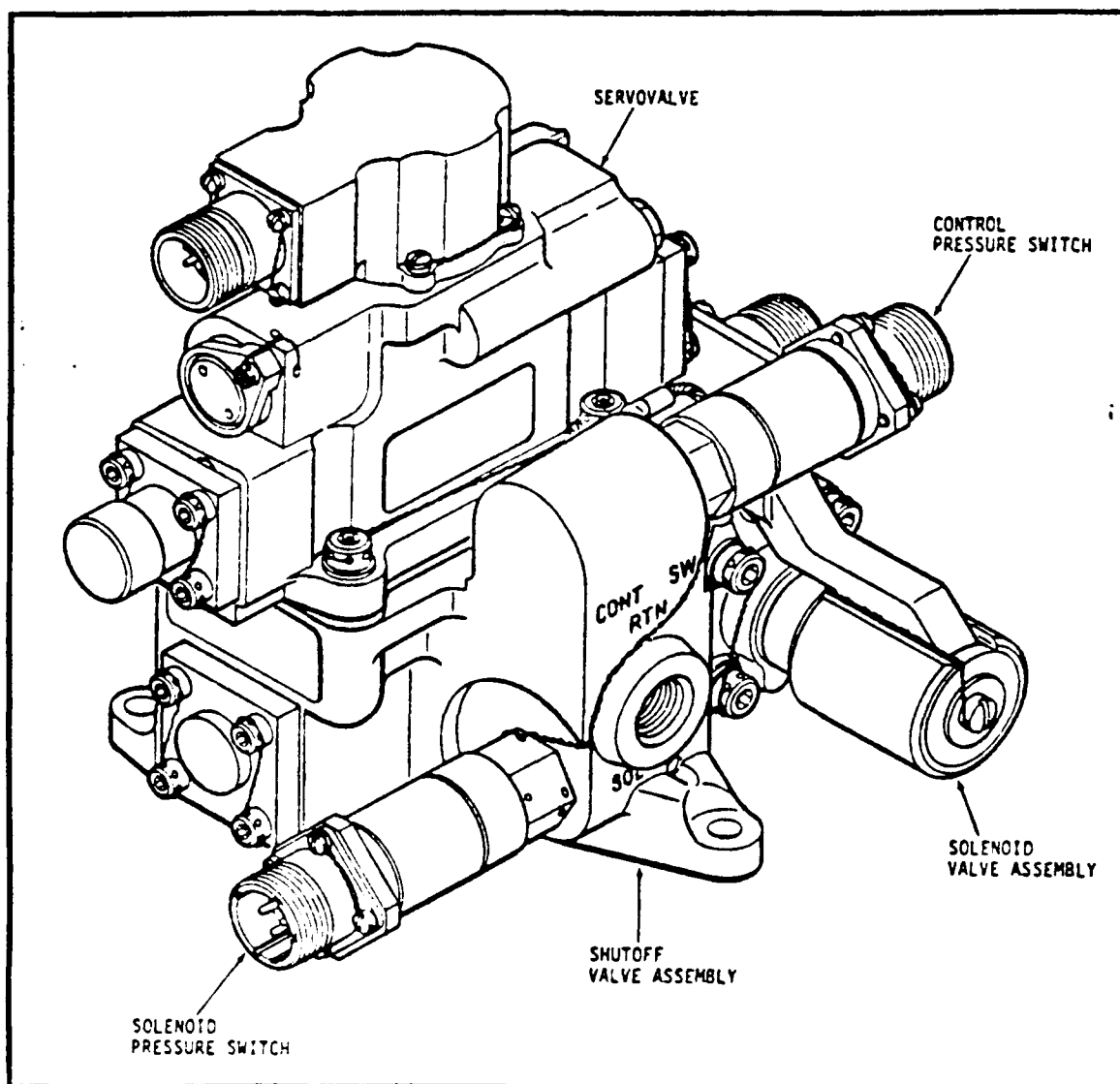


Figure 3.2-1 Pictorial drawing of the autobrake module, Type 2.

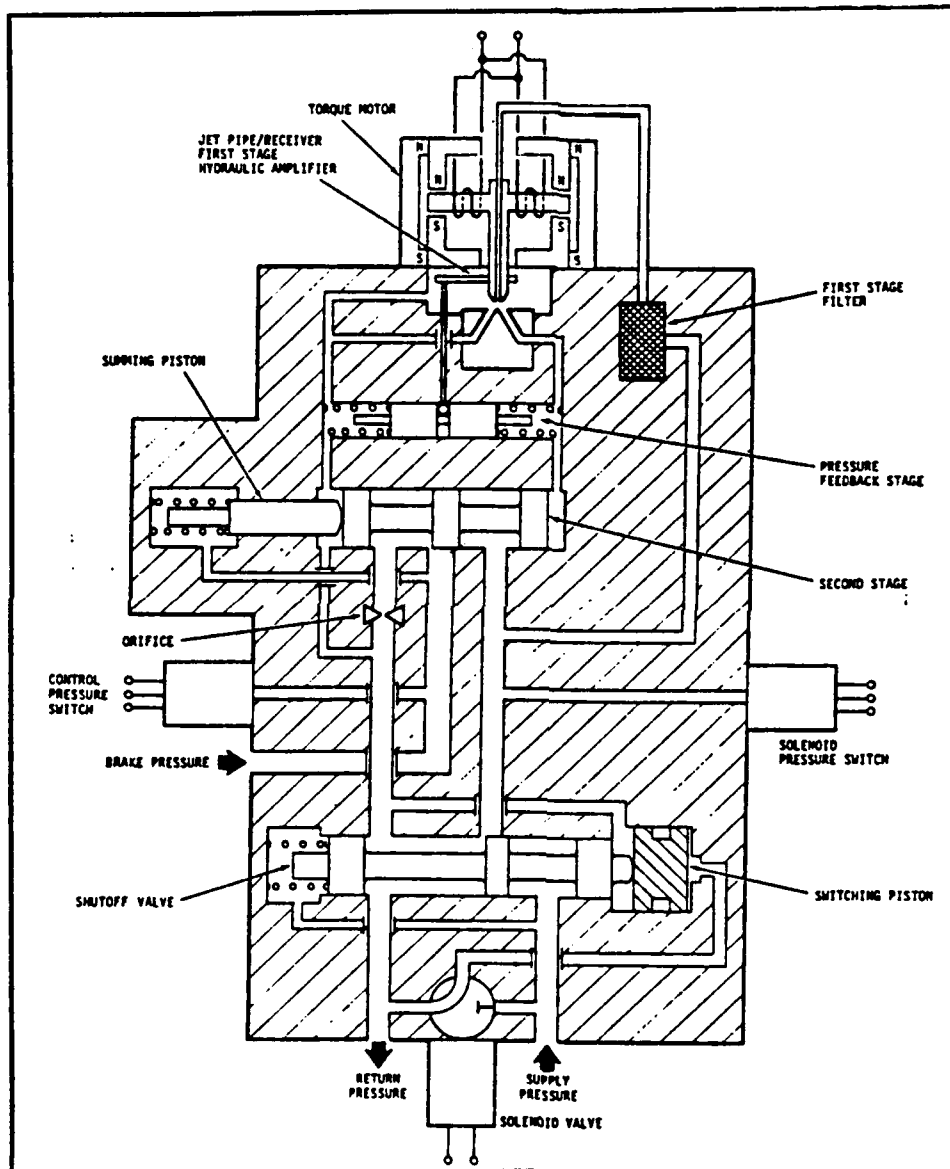


Figure 3.2-2 Schematic drawing of the autobrake module, Type 2.

The problem experienced with this type of unit was incomplete shutoff and seemed to indicate a problem with the shutoff valve assembly. Figure 3.2-3 is a breakout drawing of the shutoff valve assembly. Previous experience with X-ray radiography of this part has shown that the part is too complex to use a radiograph for investigation purposes. CT provides a means to observe the internal detail of the shutoff valve without the confusion of the complex externals. The autobrake module was brought to a medium resolution CT facility for nondestructive evaluation. A digital radiograph was taken, and CT slice heights were then selected to inspect the suspect shutoff spool valve and the other control spool valves. The first CT slice, in Figure 3.2-4 and the enlargement of the spool image in Figure 3.2-5, show that the shutoff spool valve had not returned to its seated/deenergized position. Subsequent slices clearly showed the capability to inspect the other areas of interest in the assembly. A strong possibility exists in the process of disassembly that the valve would have seated leaving no clear evidence of the failure.

CT proved to be a quick, effective way to determine the internal condition of the autobrake module. This nondestructive evaluation saved the tedious process of disassembly and notation of any and all observations that might be indicative of the problem.

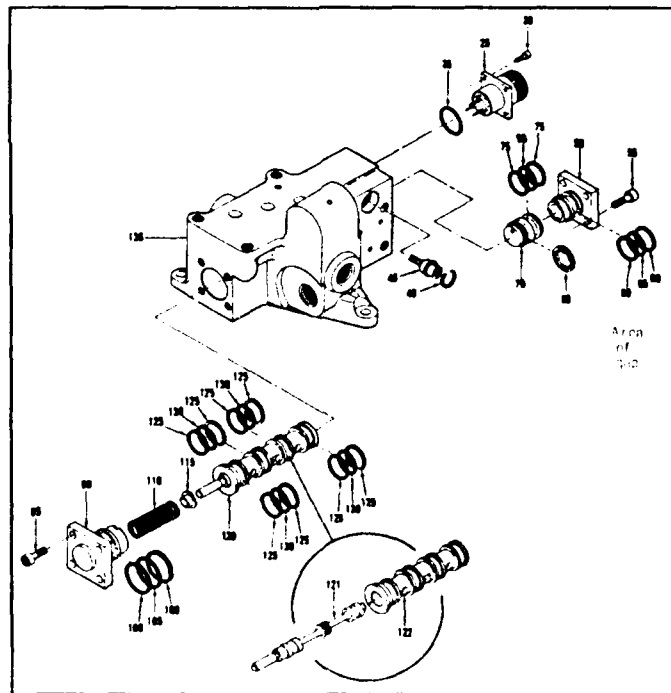


Figure 3.2-3 Breakout drawing of the autobrake module shutoff valve assembly.

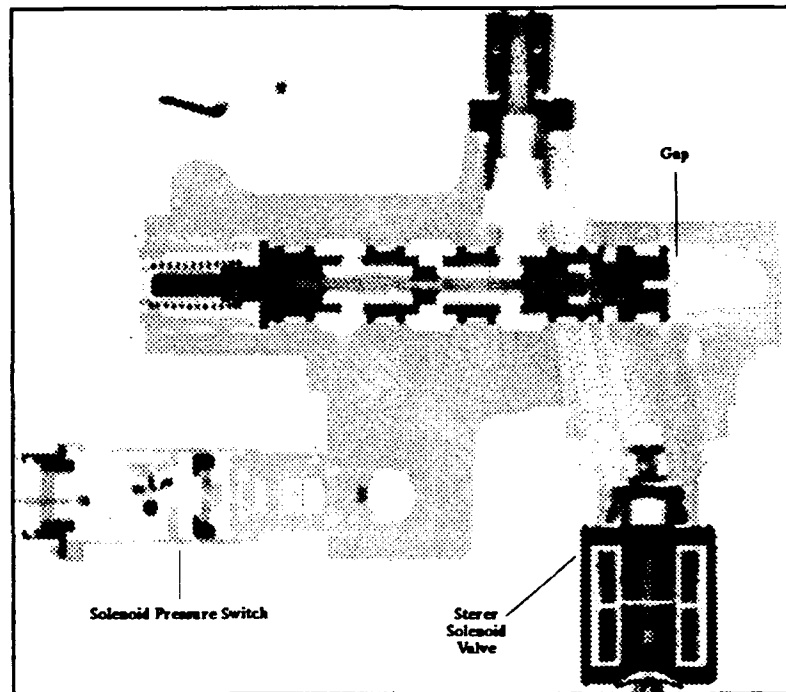


Figure 3.2-4 CT slice through the autobrake module at the height of the pressure control servovalve.

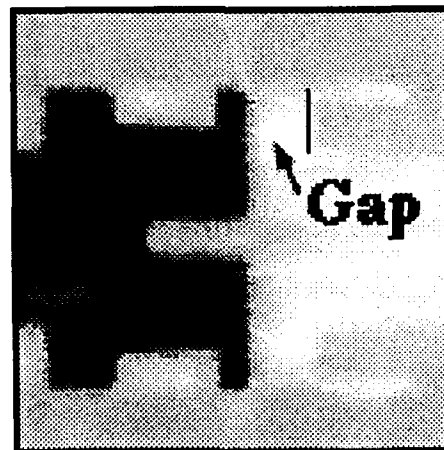


Figure 3.2-5 Enlargement of the shutoff spool valve showing gap.

3.3 Solenoid Valve

A solenoid valve, which is approximately 25 mm (1 in) in diameter is shown pictorially in Figure 3.3-1. The valve controls hydraulic pressure by an electromagnet, plunger, return spring, and ball assembly as shown in Figure 3.3-2. When deenergized the plunger and return spring hold the ball securely against the seat; when energized, the plunger is pulled away from the ball allowing the hydraulic fluid to displace the ball away from the seat and flow to the output port. A failure analysis of a solenoid valve that had been involved in a fire used CT to help evaluate the valve condition.

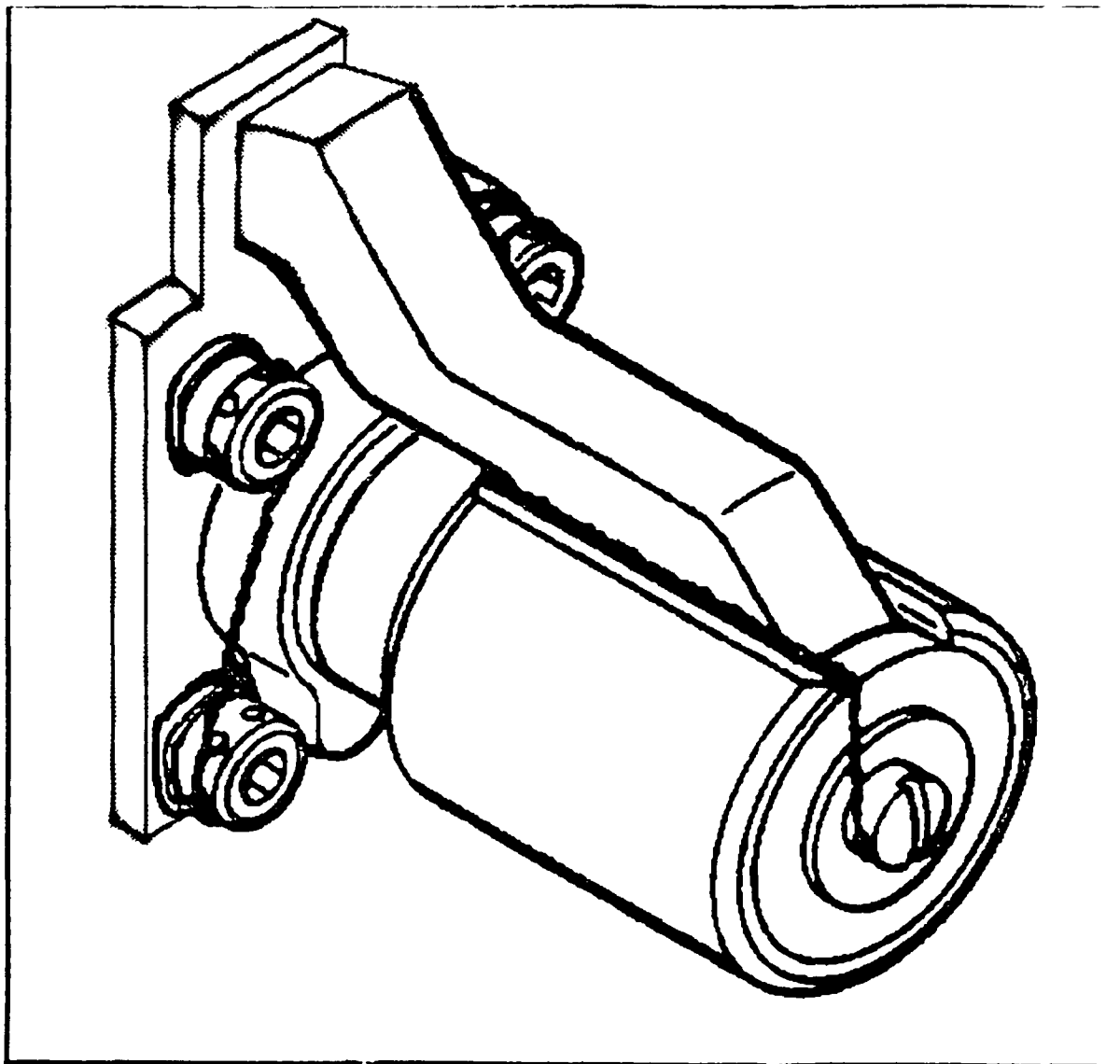


Figure 3.3-1 Pictorial drawing of the solenoid valve assembly.

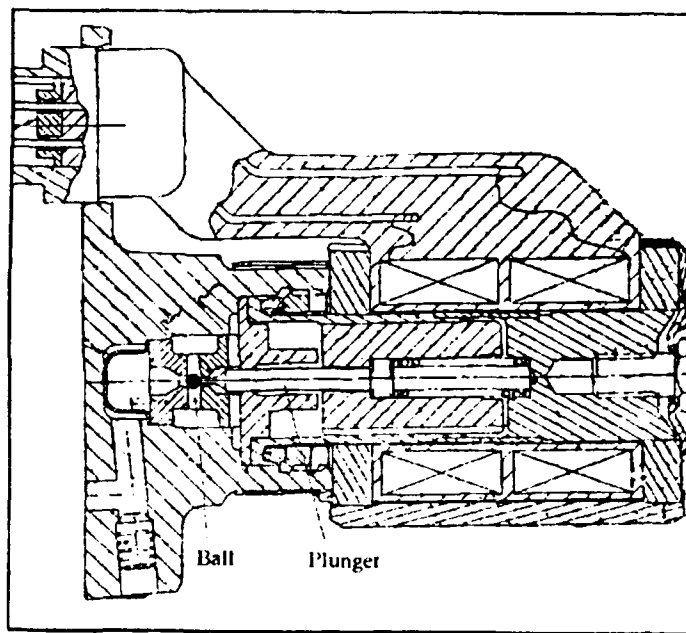


Figure 3.3-2 Cutaway drawing of the solenoid valve.

This CT scanning was performed on a medium resolution (~ 1 lp/mm) CT system. Although the component was small enough to be scanned on a much higher resolution CT system, scheduling did not allow this option. However, even the medium resolution system could show the position of the ball on the seat. Figure 3.3-3 is a longitudinal scan of the burned unit and Figure 3.3-4 is of a new unit. In these scans the interest is in observing how well the ball is seated. With the resolution available, the edge of the ball is blurred, making the interpretation of contact difficult. A new solenoid, in the closed condition was scanned as a comparison. The fact that the ball was in the normally closed position was verified to the limits of the CT system.

CT slices were also taken across the solenoid valve, through the region of the ball and seat. The new solenoid was scanned simultaneously with the burned unit so that the scans could be compared to verify that the burned unit was in the normally closed position. Figures 3.3-5 through 3.3-12 are CT slices taken through the plunger and body and then the ball and seat section of the two valves. The CT slices are in steps of 0.5 mm. Due to the heat damage and buckling of the base, these scans are offset slightly such that the burned unit on the right is slightly higher than the new unit on the left. Interpretation of these images indicates no significant difference between the burned unit and a closed new unit. The CT series measures the presence of material over the volume that is scanned. Fundamentally, the data is available to make a judgement about the position of the ball relative to the seat. However this was the first investigation of this type and with no prior experience, the CT analysis could not be definitive about the seating of the ball.

The nature of hydraulic systems is that small leak paths, even on the order of just thousandths of an inch, can be significant. Because the CT data was not definitive, there was a need to optically verify the actual seating of the ball. A destructive physical analysis (DPA) was performed and this fact was verified. Higher resolution CT and comparison to a "good" unit should be capable of the assessment of the status of the seating of the ball. Also, if the ball was not seated by any significant amount (>25 μm), it would most likely be very evident in the CT imaging, particularly in comparing a known, seated valve to an unknown.

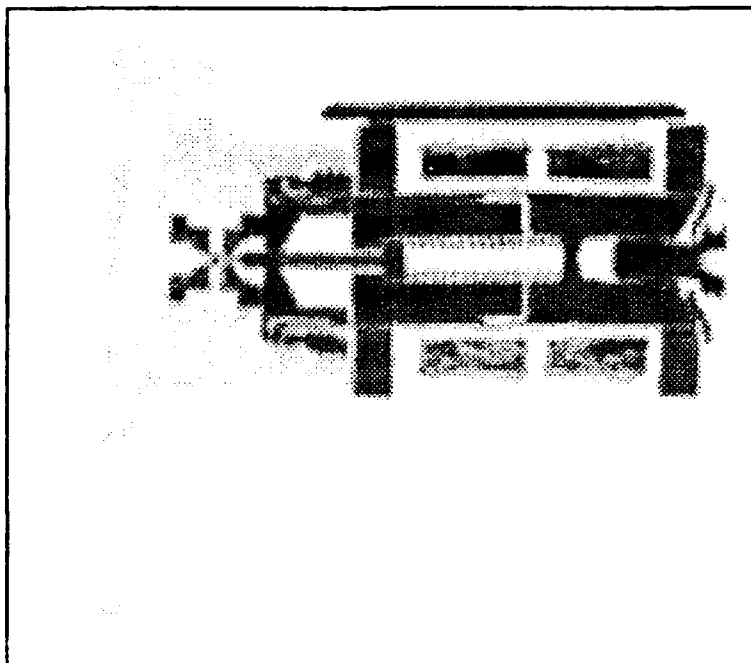


Figure 3.3-3 Longitudinal CT slice through the burned solenoid valve.

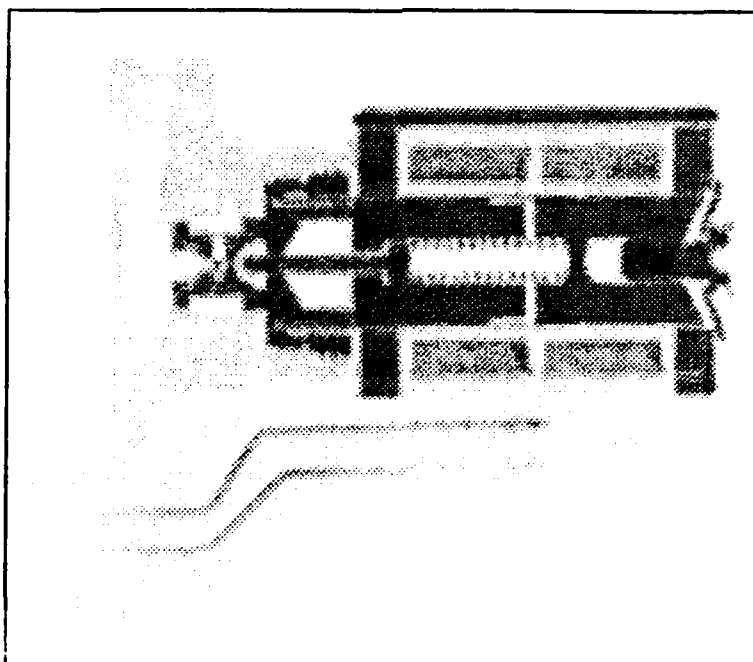


Figure 3.3-4 Longitudinal CT slice through a new solenoid valve.

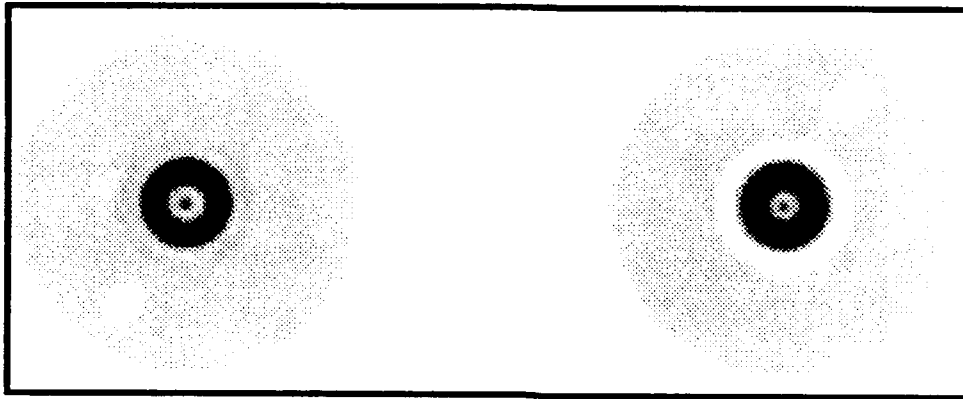


Figure 3.3-5 CT slice through the new (left) and burned (right) solenoid valves at CT system height 488.5.

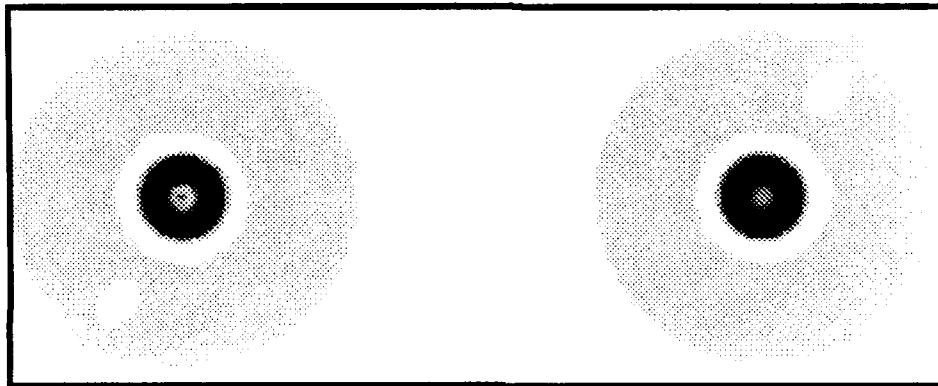


Figure 3.3-6 CT slice through the new (left) and burned (right) solenoid valves at CT system height 488.0

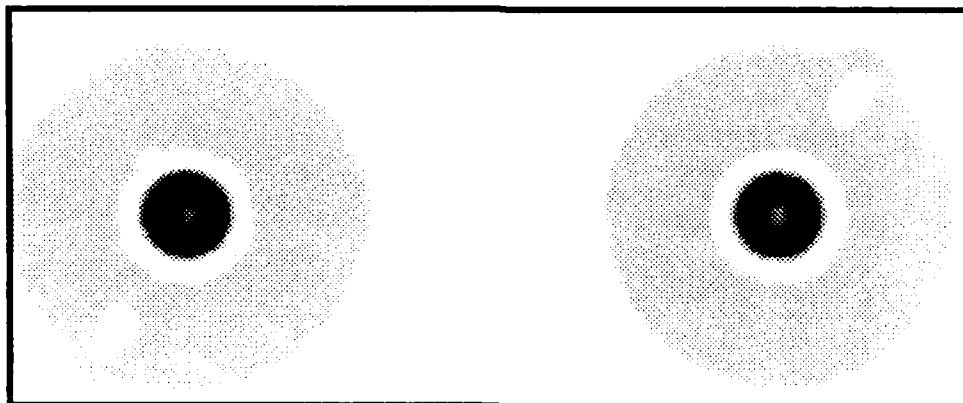


Figure 3.3-7 CT slice through the burned (left) and new (right) solenoid valves at CT system height 487.5.

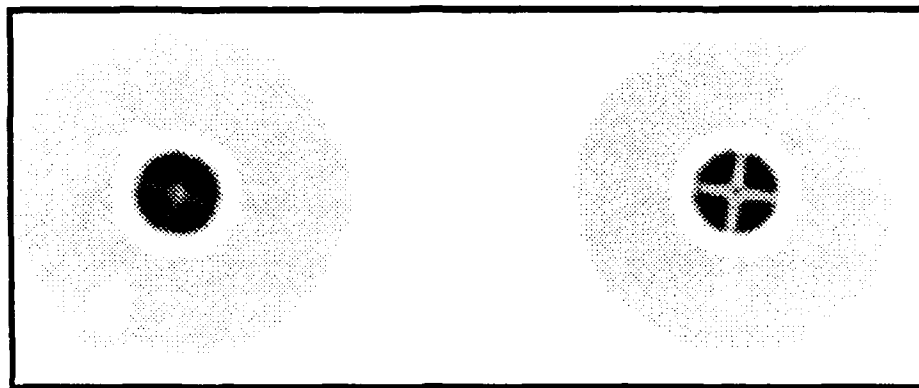


Figure 3.3-8 CT slice through the new (left) and burned (right) solenoid valves at CT system height 487.5.

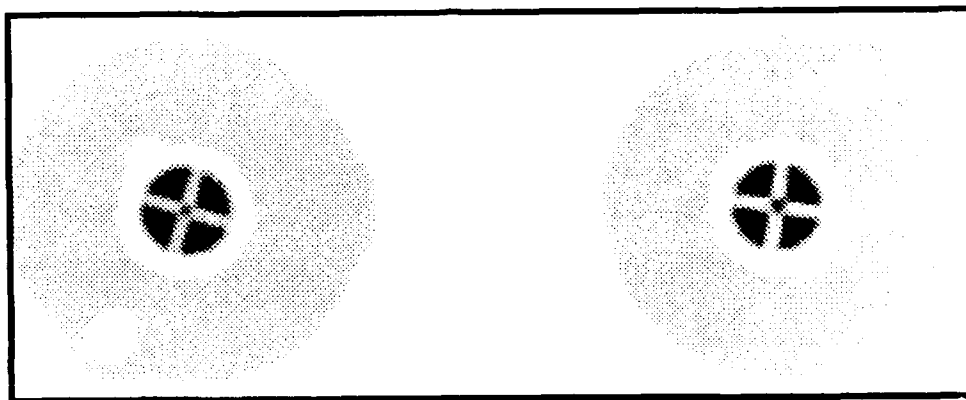


Figure 3.3-9 CT slice through the new (left) and burned (right) solenoid valves at CT system height 486.5.

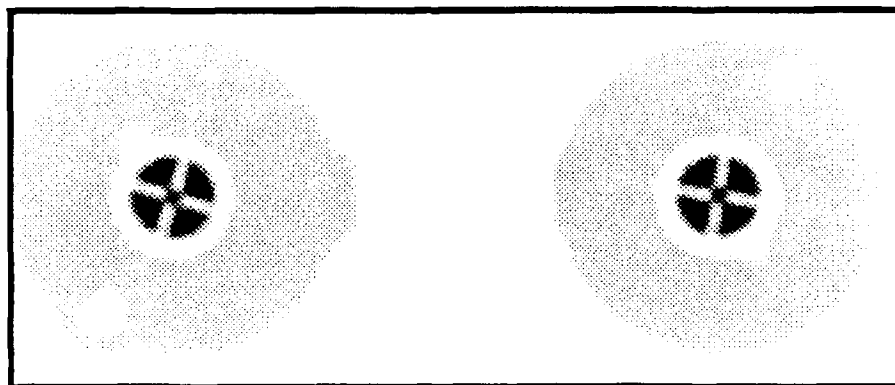


Figure 3.3-10 CT slice through the new (left) and burned (right) solenoid valves at CT system height 486.0.

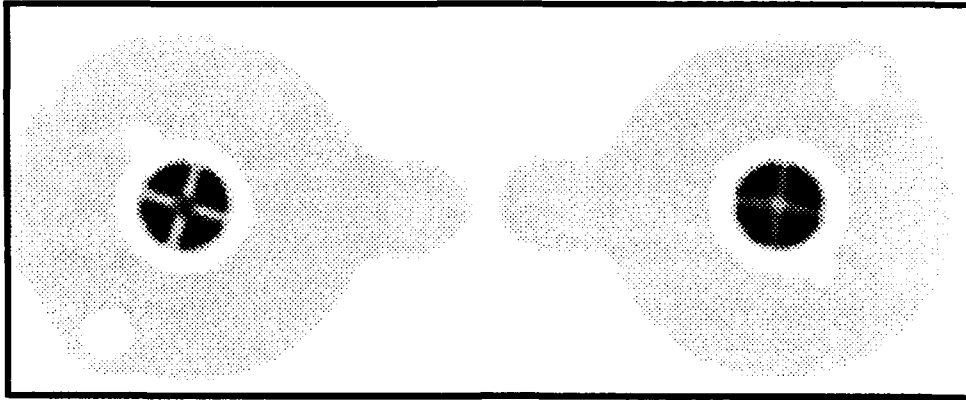


Figure 3.3-11 CT slice through the new (left) and burned (right) solenoid valves at CT system height 485.5.

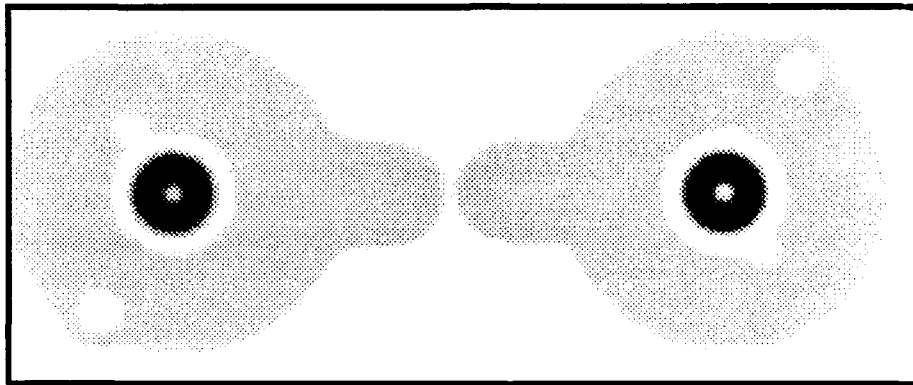


Figure 3.3-12 CT slice through the new (left) and burned (right) solenoid valves at CT system height 485.0.

4.0 ELECTRICAL COMPONENTS

Electrical components have a full spectrum of mechanical aspects and properties in addition to their electrical/electronic properties and characteristics. Many of these mechanical aspects can be responsible for a failure, such as bond wires, die attachment, die layout, packaging defects, contaminants and others. The results of the review of the 1990 workload revealed that there are two significantly large groups that CT for failure analysis does not apply to; parts removed in error during troubleshooting (they pass subsequent electrical performance tests) and parts with out-of-tolerance electrical/electronic performance owing to nonmechanical failure.

Failure analysis of small electronic components using CT was identified as an important application for high resolution CT in Task 1, "Computed Tomography of Electronics," and Task 5, "X-ray Tomographic Inspection of Printed Wiring Assemblies and Electrical Components," [1,6]. Additionally in the Task 10 effort on high resolution CT [9], small (typically <5 mm (0.12 in) in size) electronic components were also investigated. The examples in this report are larger components (>25 mm (1 in)).

4.1 Instrumentation Wafer Antenna

An instrumentation wafer antenna use in missile systems, of the type shown in Figure 4.1-1, was submitted for a physical measurement to the Parts Failure Analysis Lab. However, a DPA for a dimensional measurement could not be performed because this was a marginal part, not a failed part. Previous attempts to do the measurement by an X-radiograph had shown that the part geometry did not lend itself readily to this measurement. Although it may have been technically possible to use the radiographic approach, it would have required a complex setup and data reduction process with further difficulty in establishing the dimensional accuracy and tolerance.

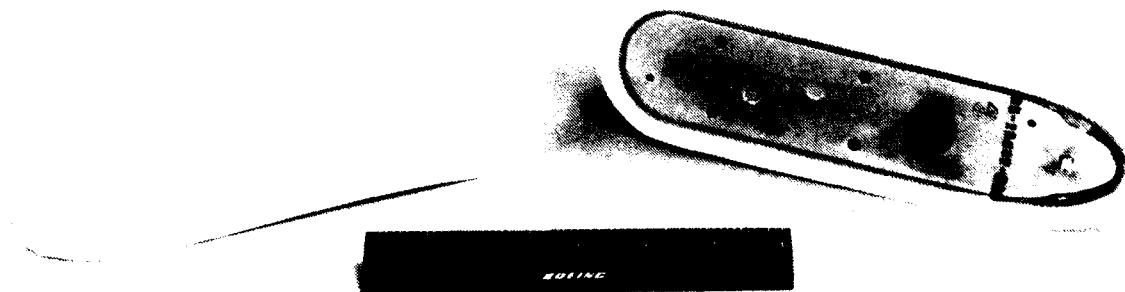


Figure 4.1-1 Photograph of an instrumentation wafer antenna.

The antenna was CT scanned, and the images show very clearly the antenna element, potting, connections and allow dimensional measurements to be readily made. Figures 4.1-2 and 4.1-3 show two CT images across the unit from two different orientations. An interactive measurement was made of the internal dimension of interest which was determined to be $14.1 \text{ mm} \pm 0.1 \text{ mm}$ (see Figure 4.1-3). This measurement supported the conclusion that the unit was performing at specification limit because of the assembly process. This was additionally supported by the fact that there were no other physical anomalies found which could have resulted in marginal performance (i.e., voids or inclusions in the potted foam or an element misalignment). The nondestructive CT measurements played a significant role in the proper disposition of this unit

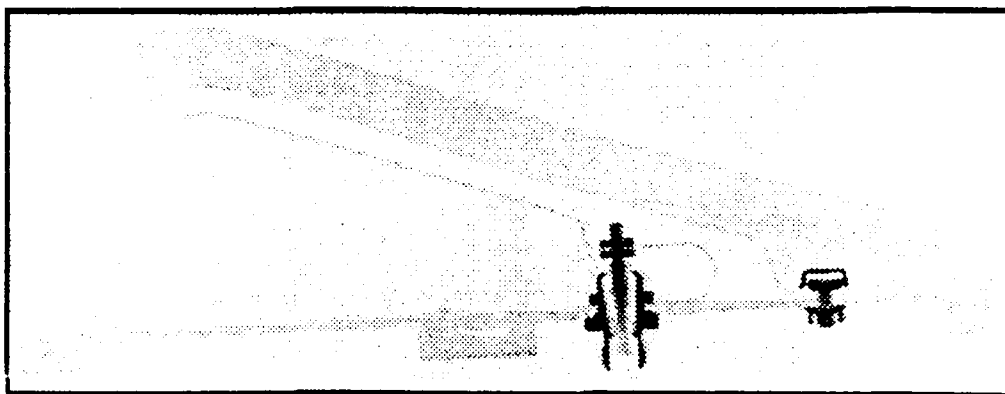


Figure 4.1-2 CT slice through the instrumentation wafer antenna.

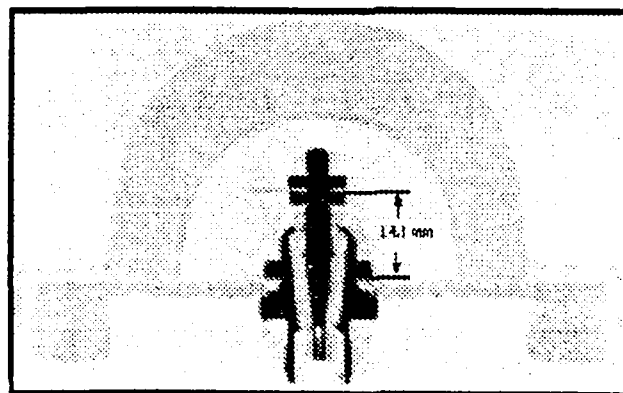


Figure 4.1-3 CT slice through the instrumentation wafer antenna.

4.2 Raceway Potted Cable Assembly

Two full-scale development raceway cable assemblies for a missile program each experienced failures during Hi-Pot (high potential insulation test). After the second cable failure, the engineering organization sought the use of CT to identify the problem and avoid DPA. (DPA on potted assemblies can be difficult to perform without destroying the evidence desired.)

The first failed cable was CT scanned in a nine-slice CT series on steps of 1 mm. This scanning sequence covered a discolored region on the cable. Figure 4.2-1 is one image from this series. This image shows where the twisted pair on the thin side (pointed end of the trapezoid cross-section) edge had been compressed over about a 2-mm (0.08-in) length. The compression is a likely cause of insulation thinning which would have resulted in the Hi-Pot failure. The CT image also shows that there is marginal room in this assembly for the number of wires required. The wires are pushing the outside envelope of the potting; in addition the narrow edge does not have adequate room for the twisted pair. This is going to be a recurring problem area for damage from manufacture and handling for this design. Figure 4.2-2 is a CT slice taken near the termination of the cables to connectors. The image indicates a poor distribution of wires in the cable as noted by the large region containing no wires.

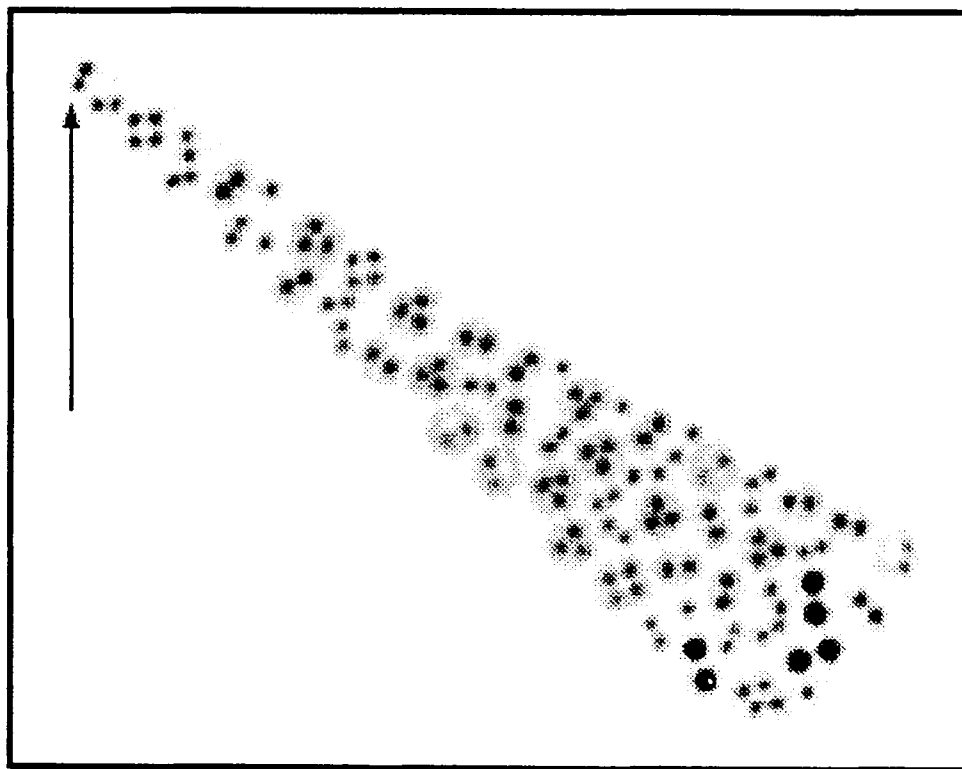


Figure 4.2-1 CT slice through the raceway cable in a region of surface discoloration for a failed cable.



Figure 4.2-2 CT slice through the raceway cable near the termination of the cable at the connector.

On the second raceway cable assembly, a visible void existed at the site of the HiPot failure. The most probable cause of the failure is that the transition from the flat portion to the end block results in excessive density of conductors and compression of insulation and wire pairs. A solution to these cable problems, worked out in an informal brainstorming session while viewing the CT data, is to increase the available space in the cable by using the 1-mm (0.050-inch) margin and adding a wrap of woven material around the outside of the wire bundle. This would provide a standoff to the external conductive shield which is sprayed onto the outside of the potted urethane. In addition, this will provide the cross-cable support to avoid the lengthwise splitting that can be the result of handling on this type of assembly. There also is a need to change the transition from the flat length of the raceway cable to the end block connectors so that there is a gradual tapering to allow more room for the transition and, which will reduce the conductor density (Figure 4.2-2). These changes would result in a reduction of approximately 50 percent of the current failures experienced and most of the observed failure modes.

In the design of potted cable assemblies there are a multitude of factors considered such as shielding, signal type, conductor density, protection and routing. Because of the nature of potted assemblies there are no hard brackets or separators to control the wires internally and this would defeat much of the flexibility of potted assemblies. Instead wires are positioned and formed to control their location. CT is the ideal tool to evaluate the success of the "layup" process because it provides the cross sectional distribution of the wires in the cable.

5.0 MECHANICAL

Mechanical devices depend on the materials selected, structural design, dimensions used, and proper assembly to achieve the desired application. Both macro and micro details are important. CT can be used as an investigation tool capable of supporting failure analysis and evaluation by providing dimensional, density and defect information. This can be accomplished at the macro level on complete assemblies and at the micro level on reduced size specimens.

5.1 Drag Brace with Experimental Bearing

A drag brace with bushings, at both ends, centered in elastomeric collars is shown schematically in Figure 5.1-1. The bushing and multilayered elastomeric material with metal shims are a new shock cushioning bearing design for the drag brace, replacing conventional bearings. Evaluation of this new system must be performed periodically to ensure that it is meeting design goals. Previous attempts to evaluate the condition of the new bearing system had required DPA and resulted in the destruction of much of the information in the process.

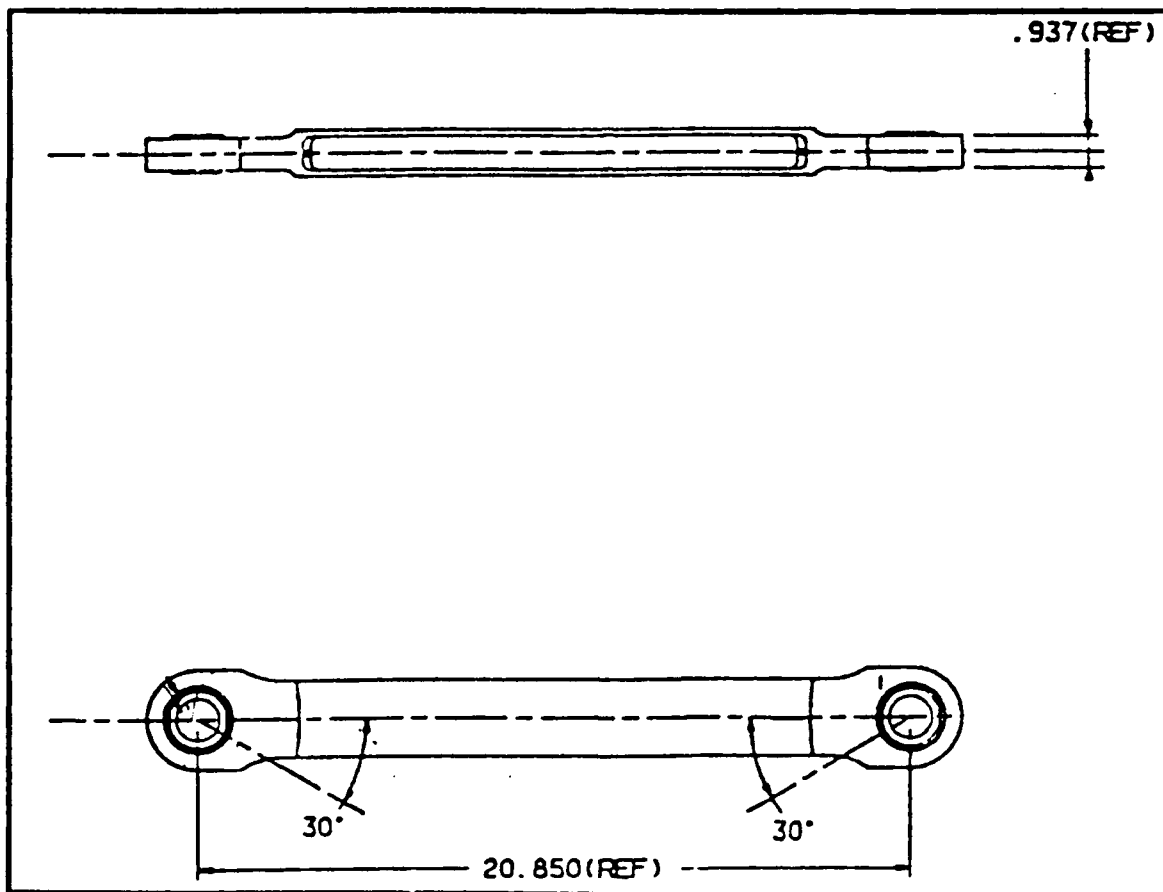


Figure 5.1-1 Drawing of the drag brace.

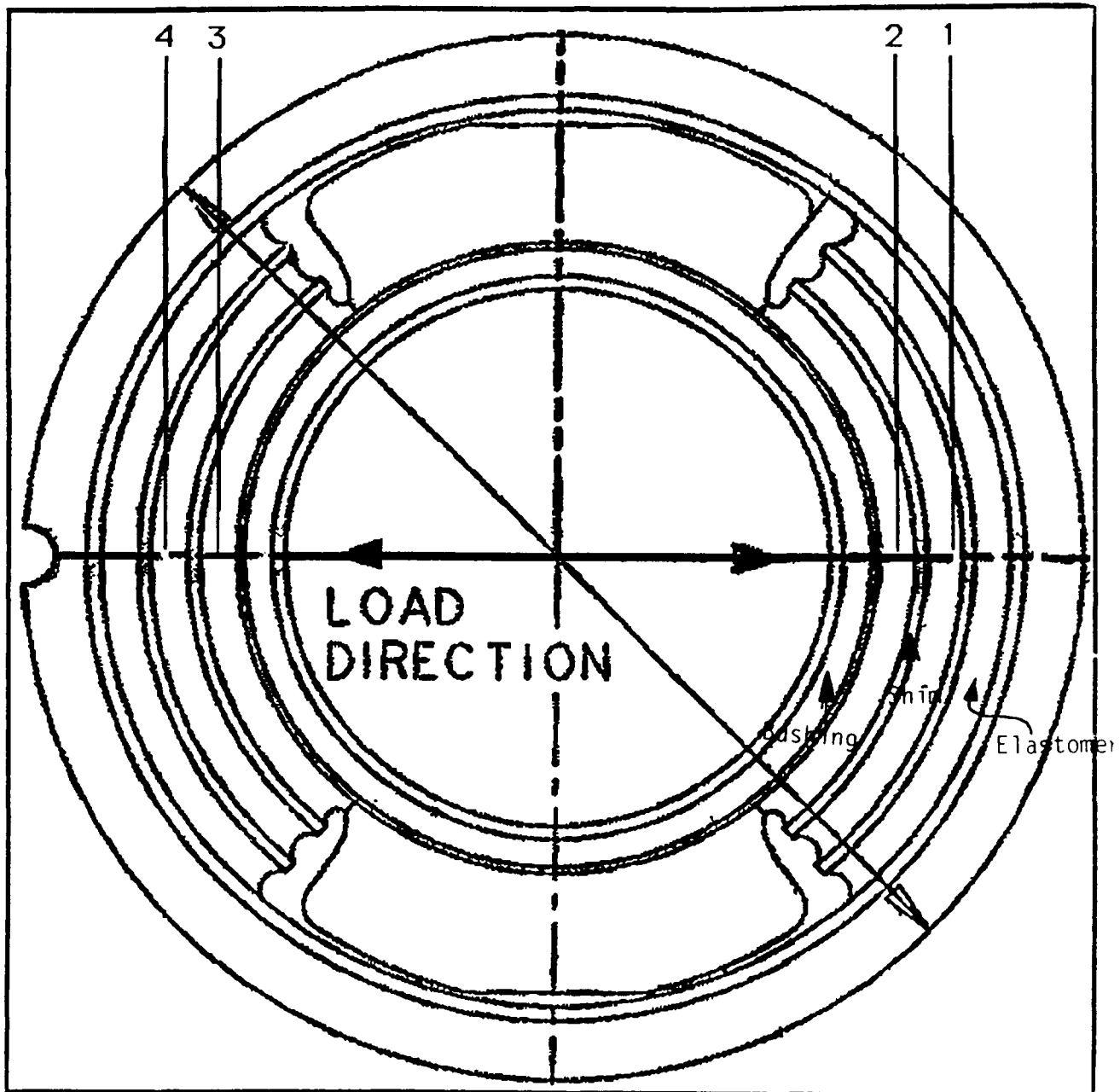


Figure 5.1-2 Schematic drawing showing the location of CT slices 1, 2, 3 and 4 on the drag brace bushing.

Computed tomography allows the observation of the interior of the new design without destructive sectioning that may relieve stresses. Figure 5.1-2 is a schematic of the elastomeric bushing which fits into the drag brace. The figure shows the location of the desired slices in the multilayered structure. Figure 5.1-3 shows the side view of this new bearing assembly design. Cylindrical section metal shims are embedded in the elastomer (to prevent it from ballooning out). CT slice locations were selected from digital radiographs of the drag brace. Figures 5.1-4, 5.1-5, 5.1-6, and 5.1-7 are CT slices taken at locations 1 through 4 respectively. The images show that the cylindrical metal shims in the elastomer have been distorted. Ideally they would appear as rectangular details in slices with this orientation. The characteristic "saddle" shape exhibited by the shims is a trait of a side load applied to this bushing which has left the material distorted. This information was supplied to the bearing manufacturer and will be used for future design changes.

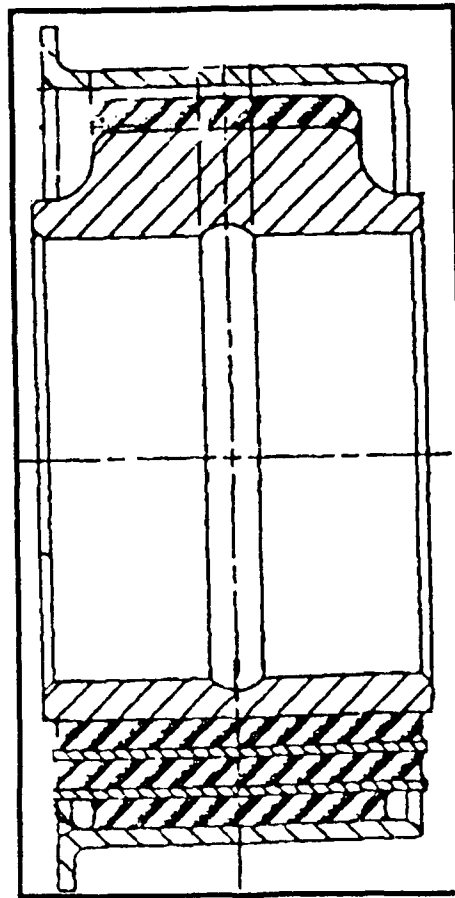


Figure 5.1-3 Cross-section drawing of drag brace elastomeric bushing assembly with 0 and 90 degree cuts through Figure 5.1-2.

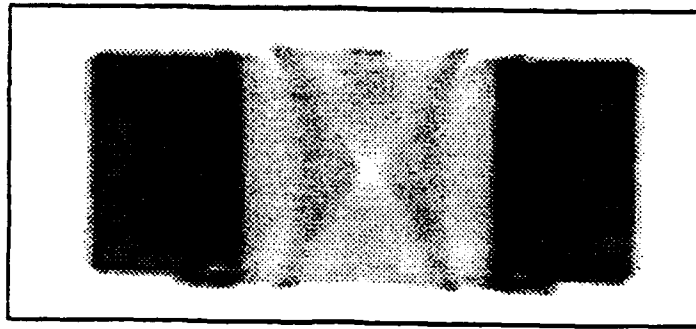


Figure 5.1-4 CT slice at location 1 on the drag brace bushing.

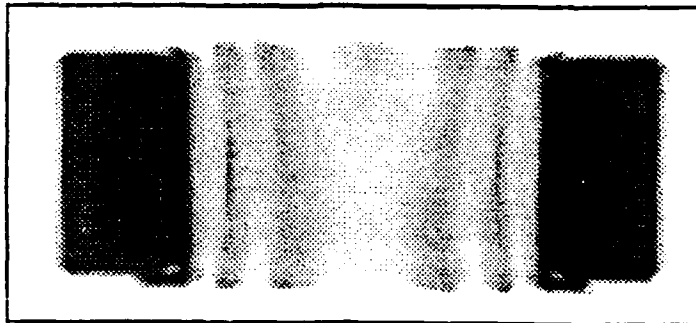


Figure 5.1-5 CT slice at location 2 on the drag brace bushing.

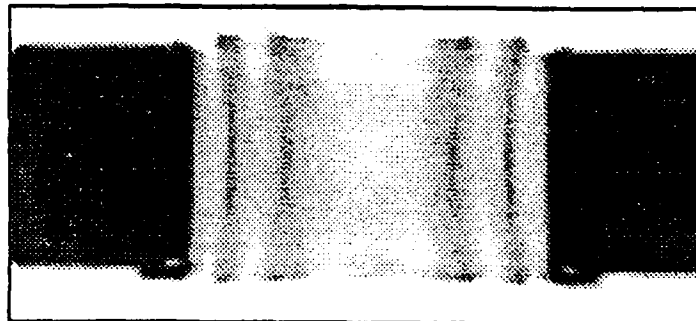


Figure 5.1-6 CT slice at location 3 on the drag brace bushing.

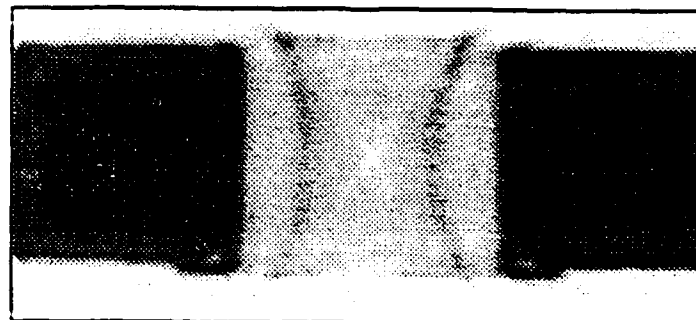


Figure 5.1-7 CT slice at location 4 on the drag brace bushing.

5.2 Fuel Line

A fuel line for a jetliner was under investigation for the possibility of collapse which would explain engine malfunction. CT was performed for nondestructive evaluation of the fuel line, and the CT test configuration was arranged so that the fuel line could be under environmental conditions. The first condition was under vacuum, the second condition was ambient pressure, and the third condition was at full operational pressure using nitrogen gas.

Figure 5.2-1 is a CT image of the fuel line at the maximum point of crush under vacuum, Figure 5.2-2 is at the same location at ambient pressure, and Figure 5.2-3 is the same location at full operational pressure. The CT images show how the inner and outer tubes behave relative to one another under the three pressure conditions. From this set of CT images, it was concluded that this fuel line could not have collapsed, and the ultimate finding of the investigation was that it was another section of fuel line that collapsed, causing the engine malfunction.

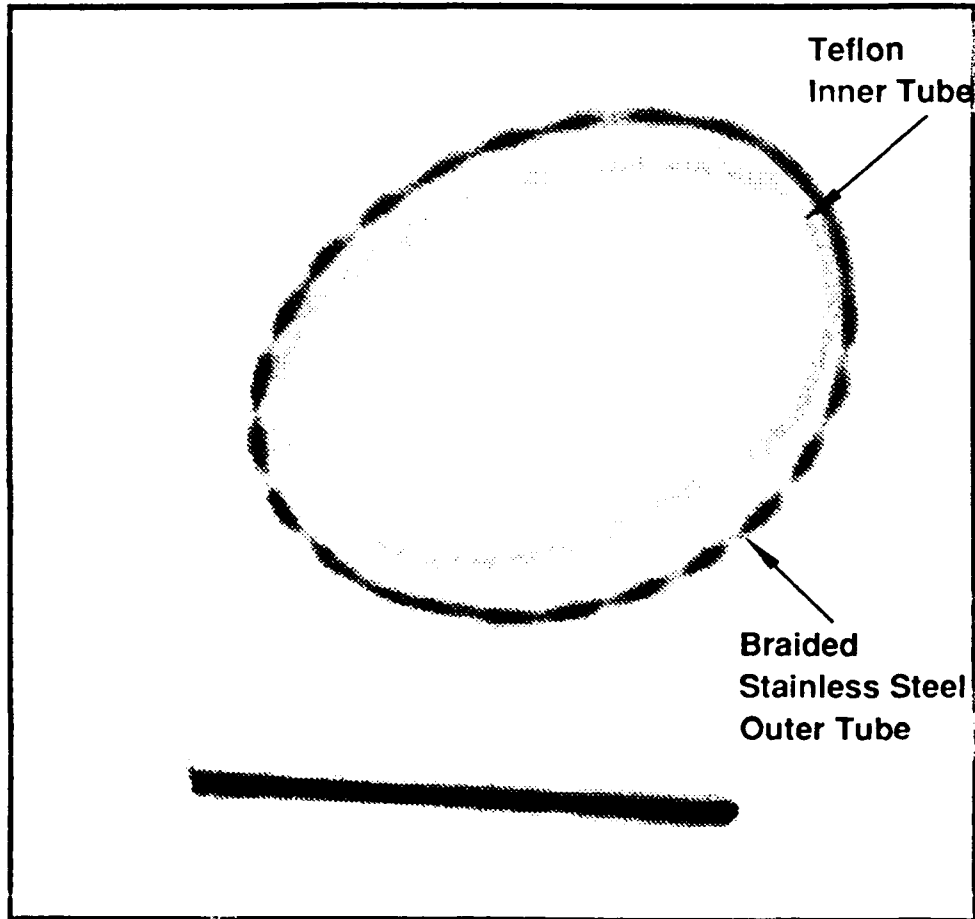


Figure 5.2-1 CT slice of a fuel line under vacuum conditions (2X actual size) showing teflon inner tube and braided stainless steel outer tube.

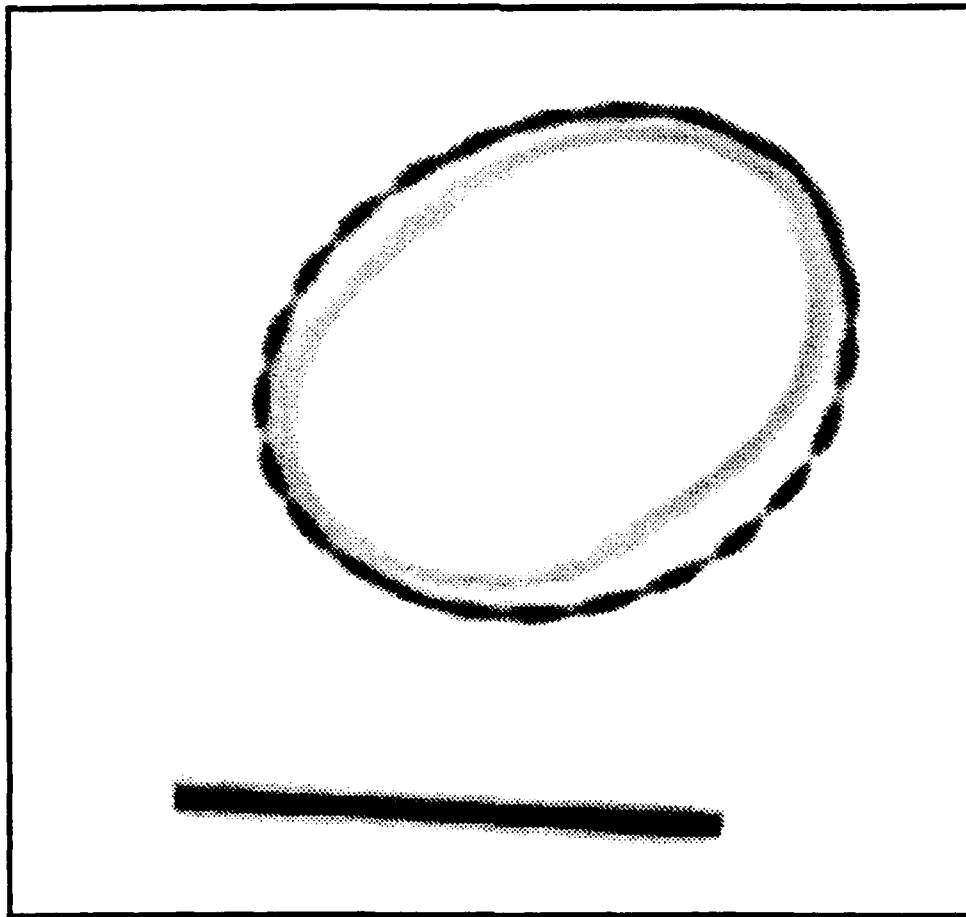


Figure 5.2-2 CT slice of the fuel line under ambient pressure.

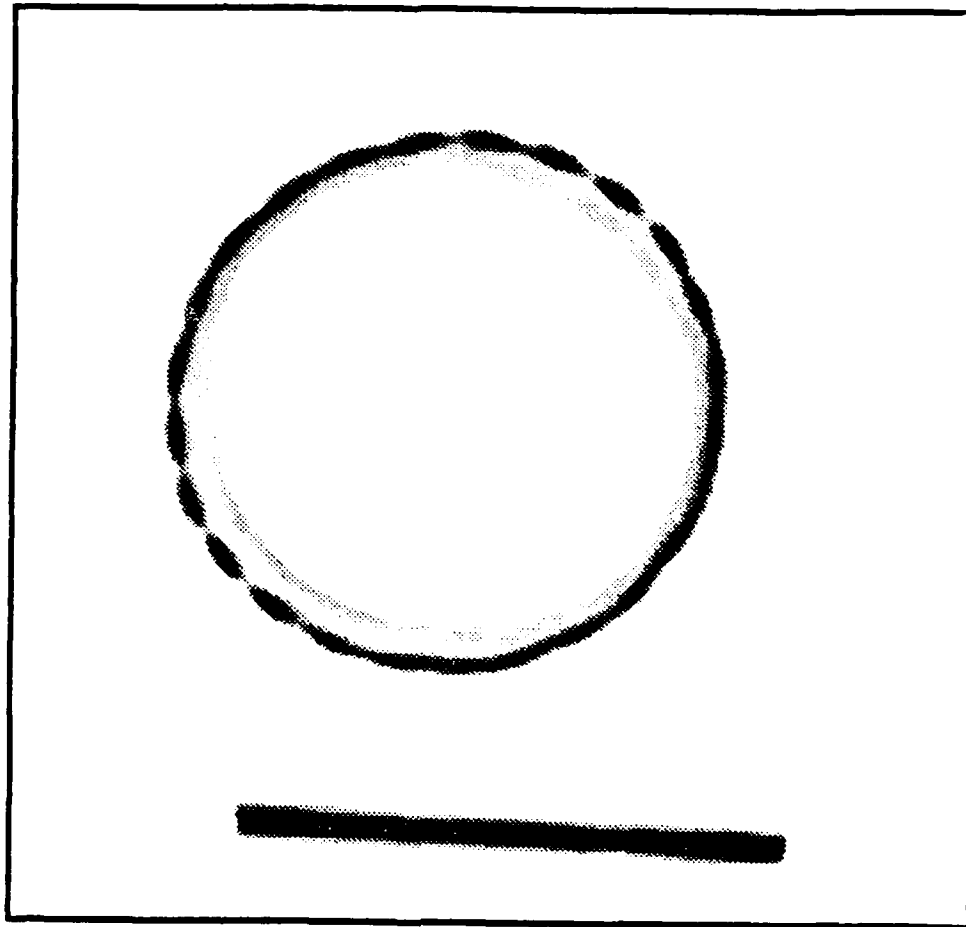


Figure 5.2-3 CT slice of the fuel line at operational pressure.

The application of CT to objects under varying or varied environmental conditions is an excellent approach to a number of investigations. CT is capable of detecting changes in dimensions (often down to the range of 25 to 100 μm (0.001 to 0.004 inch)) which occur during pressure, temperature, activation, motion or loading conditions that a component or system might experience in service or testing. Internal parts which move relative to each other are easily monitored, noninvasively. CT systems are normally capable of handling the additional apparatus needed to provide the environmental conditions, such as pressure lines, ovens or loading cell, and such apparatus can be designed to be used with minimal interference with the CT imaging [10].

6.0 MATERIALS

Components fail when the external loading exceeds the strength of one or more of its constituent materials. The failure may be due to a loss of strength of a constituent material, or the operating stresses are raised above a critical strength. The degradation of material properties through such phenomena as fatigue cracking, erosion, oxidation, and improper manufacture can result in failure. Excess stress, temperature, vibration, or pressure can also cause failure, either by degrading the material properties, or by subjecting the component to stresses which exceed the inherent strengths. Determination of the initiation sight and understanding the actual cause of an unplanned failure is critical to preventing future failures. Failure mode evaluation of destructively tested specimens is very important for the development of a new material.

Because it may be one of a number of possibilities, the cause of failure in complex systems (such as some composites and other advanced materials) is usually determined through time-consuming and costly evaluation methods such as destructive sectioning, microscopy, and chemical analysis. CT can be a supplemental evaluation tool, and in some cases, an alternative tool for failure analysis of materials. It provides the capability of examining the interior of a material system before or in lieu of destructive sectioning, and allows quantitative measurement of dimensional and density information.

6.1 Failure Analysis of Honeycomb Panel

Figure 6.1-1 is a photograph of a 150-mm x 225-mm (6- x 9-inch) graphite/epoxy honeycomb panel with a Ti alloy core. The panel was loaded to failure by an unknown method as part of a blind test of composite failure analysis capabilities. CT was chosen as a nondestructive evaluation tool to assist in the analysis.

The panel was scanned on a medium resolution CT system at the locations shown in Figure 6.1-2. A series of 14 contiguous slices on a spacing of 2 mm were taken through the middle section, providing a 3-dimensional data set 28 mm thick. A slice near the center of this delaminated region (slice location A) is shown in Figure 6.1-3. It shows multiple delaminations that extend most of the way across the part. Figure 6.1-4 is the same image, but the grayscale levels are set to show the detail in the honeycomb core. The walls of the core are clearly buckled on the outer edges of the panel. There is also a slight bend in the core, with the concave side facing up.

Three CT slices (locations B, C, and D) were taken in a direction perpendicular to the slice A series as shown in Figure 6.1-2. One was taken down the center of the panel (slice C), and the other two, approximately 19 mm (0.75 inch) from each edge (slices B and D). Figure 6.1-5 shows the cross-sectional image produced at slice B. Rotation of the core walls due to shearing of the right half of the core can clearly be seen. Also, peeling of the core away from the lower skin is indicated in the lower right hand corner. This type of phenomenon would occur if the top sheet were sheared to the left relative to the bottom skin. The center region shows multiple delamination which indicates compressive loading along the face of the top plate. The left half of the panel did not undergo shear deformation. Figure 6.1-6 is a 2x magnification of the left side of the same image. The cores at the left end of the image reveal a slight kinking in several of the core walls, indicating a compressive loading perpendicular to the panels near that edge.

Figure 6.1-7 shows the left half of the image from slice location D. The features are equivalent to those identified in Figures 6.1-5 and 6.1-6. The only difference is that the kinking in the core walls is slightly more prominent and extends across the length of the left side.

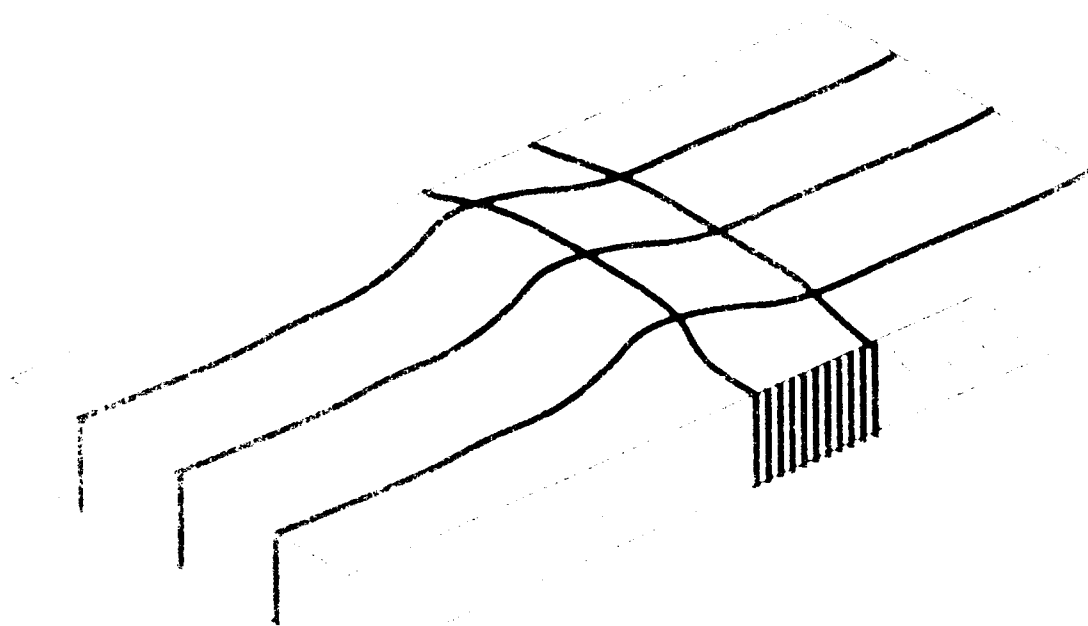
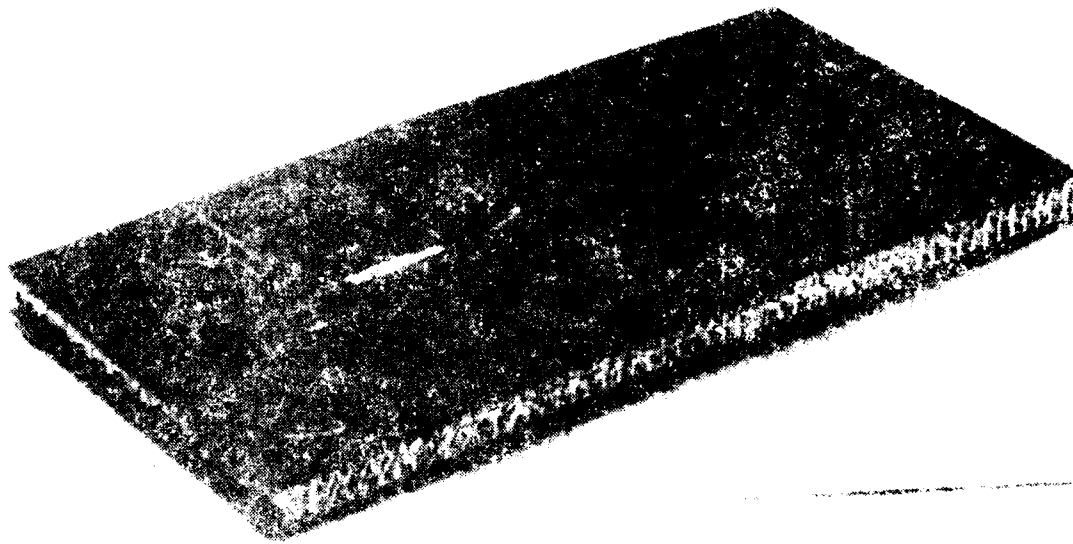




Figure 6.1-3 CT slice at location A.

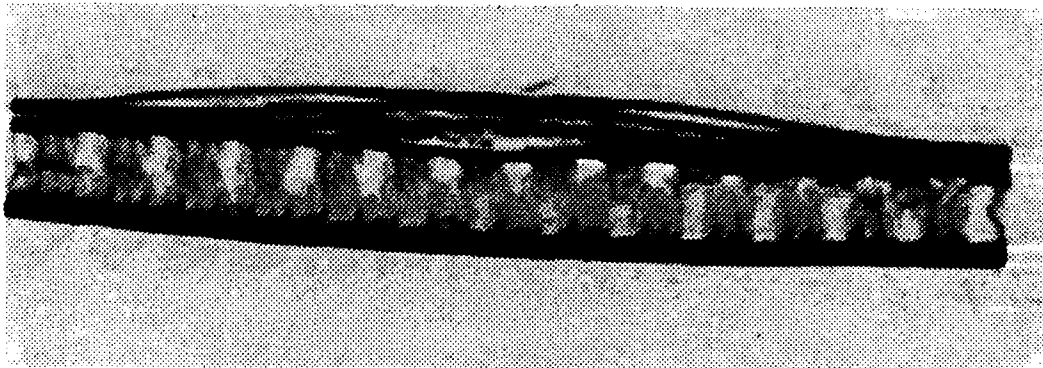


Figure 6.1-4 CT slice at location A with gray scale in image adjusted to observe the honeycomb.



Figure 6.1-5 CT slice at location B.



Figure 6.1-6 2x enlargement of CT image at location B.

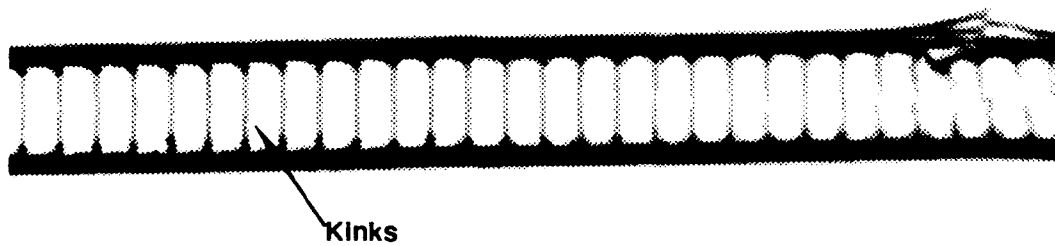


Figure 6.1-7 CT slice at location D.

Figure 6.1-8 shows the left half of the image from slice location C. The features are again equivalent to those from the previous two slices. The kinking of the core is again seen on the left hand side of the image.

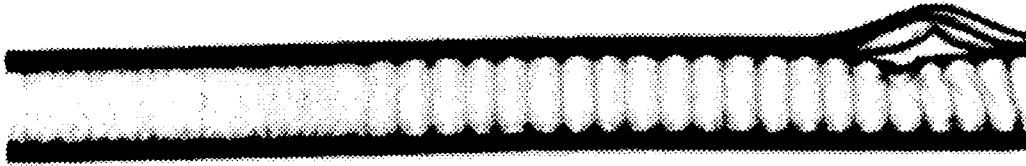


Figure 6.1-8 Left half of the CT slice at location C.

The delaminated region in Figure 6.1-8 is very interesting. While the outer layers have formed a smooth bulge, an inner layer can be seen that forms a cusp. This possibly indicates a discontinuity in the plies at this point, which may why the delamination failure occurred in this region.

Based on the sum of CT results, most likely the panel was loaded in compression along its long axis. The shearing in the core would be caused by selective loading of only one skin, as shown in Figure 6.1-9. Bending of the panel might also cause the shearing, but evidence of fracture on both skins would be expected. Ample evidence suggests that the part was held in some type of frame when it was loaded, as shown in Figure 6.1-10. The slightly kinked cores shown in Figures 6.1-6, 6.1-7 and 6.1-8 could be explained in this way. The fact that the kinks extend along the entire left half of the sample in Figure 6.1-7 means that the scan at location D was probably entirely in the region that was in the frame. Other evidence of the frame is the relative lack of delaminations near each edge (see Figure 6.1-4). External visual evidence also suggests a frame. Traces of a rubbery adhesive were observed on the part in several places where the frame may have ended.

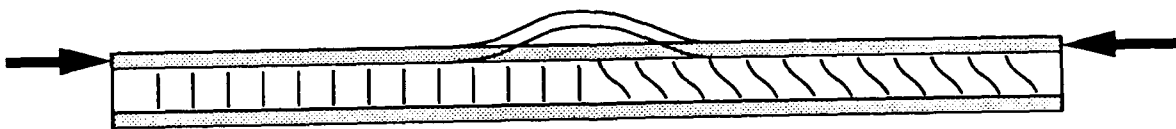


Figure 6.1-9 Schematic of suggested selective loading of honeycomb panel.

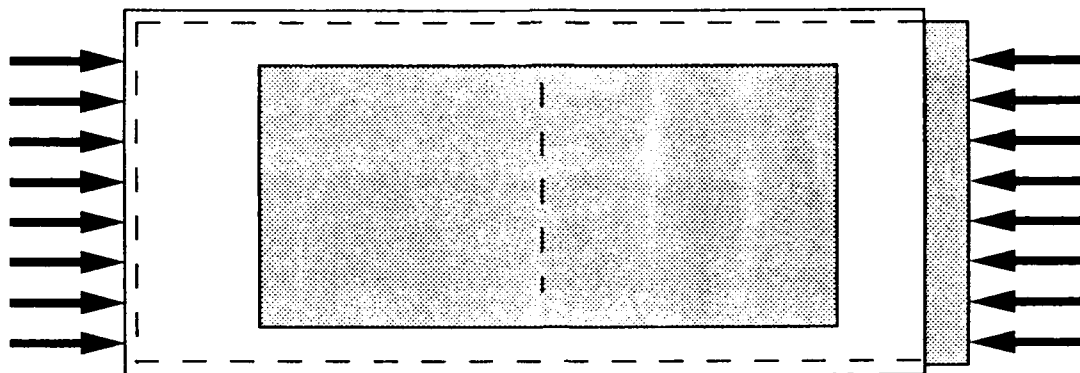


Figure 6.1-10 Schematic of the frame constraints for loading of the test sample.

The fact that the panel failed where it did may be due to a discontinuity in the plies at this point. There may also be a lack of adhesive in this center region, though CT was not able to determine whether or not this is true.

On the basis of these results, it was suggested that the center delaminated region be tested for ply discontinuity and lack of adhesive. Also, a modified alcohol wipe* was also recommended for the outer faces of each plate to determine if there is further evidence of indentation. It was also suggested that a complete volumetric CT data set (about 50 CT slices) could be made, and the results could be viewed on 3-D imaging software. Such an analysis would allow a better interpretation of the extent of the compression loading indicated on the left end of the panel.

* A modified alcohol wipe uses mixture of 50 percent alcohol and 50 percent water. The wiping of the mixture on the surface of a component enhances the visual detection of surface damage during inspection. This technique is used on composite exit cones.

6.2 Composite Damage Analysis

The assessment of damage in composite structures can be difficult. If destructive analysis is performed for assessing the damage, then each layer of the composite must be carefully removed and the surface photographed to determine the extent of damage on each layer. In an earlier task report [9] it was shown that high resolution CT systems could image features less than 0.1 mm in size (0.004 inch) in samples less than 25 mm (1 inch) in size. An example of applying this capability to composite damage is the photograph of a composite impact damaged test sample and a coupon extracted from the impact region of the sample shown in Figure 6.2-1. Figure 6.2-2 is a CT image through the center of the coupon showing the characteristic delamination pattern due to impact damage.

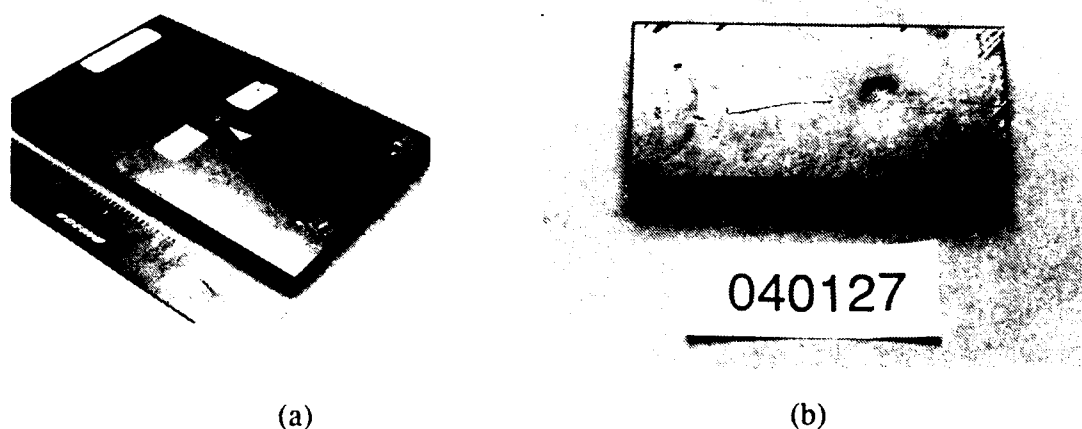


Figure 6.2-1 Photograph of the graphite epoxy composite sample a) impacted test panel, b) small coupon removed from the damaged region.

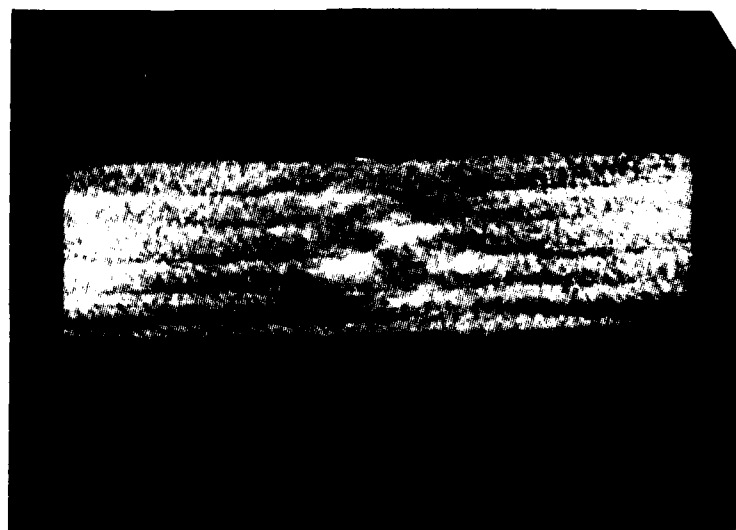


Figure 6.2-2 CT slice through the center of the impacted coupon showing delaminations.

This capability can be useful when assessing the internal damage of failed structures. An example is the understanding of damage around a fastener hole in a failed structure. Figure 6.2-3 shows a CT slice from a graphite epoxy coupon of 22 x 18 x 45 mm. This particular slice indicates a transverse crack and a zero degree crack which intersect the fastener hole.

For this particular sample evaluation, radiopaque penetrant had been added to the sample to enhance radiographic definition of the cracking. The penetrant however did not enter all delaminations and cracks in the sample. In the CT data, the cracks and delaminations appear as higher density indications where the penetrant is present and lower density indications where there is not penetrant. In order to evaluate the distribution of cracks and delamination throughout the sample, that could appear as light or dark indications, the data was mathematically processed using mathematical morphology [11]. The mathematical morphology approach uses techniques to extract information based on the feature shape, so that the cracks and delaminations (as either higher or lower density indications) can be separated from noise in the image.

By applying morphological processing the cracks and delaminations present in the component were extracted in binary image data form. This processing was applied to a series of CT images to form a three-dimensional model of the failure locations throughout the sample. Figure 6.2-4 is a 3D model of the failure area of the specimen created from the data set. The single view shown here does not do the 3D imaging justice, compared to viewing the model on a video screen that allows real-time rotation of the image and observing the features from multiple viewing angles. This model of the failed specimen provided valuable insight on the specimen and served as a guide for further destructive micrographic analysis.

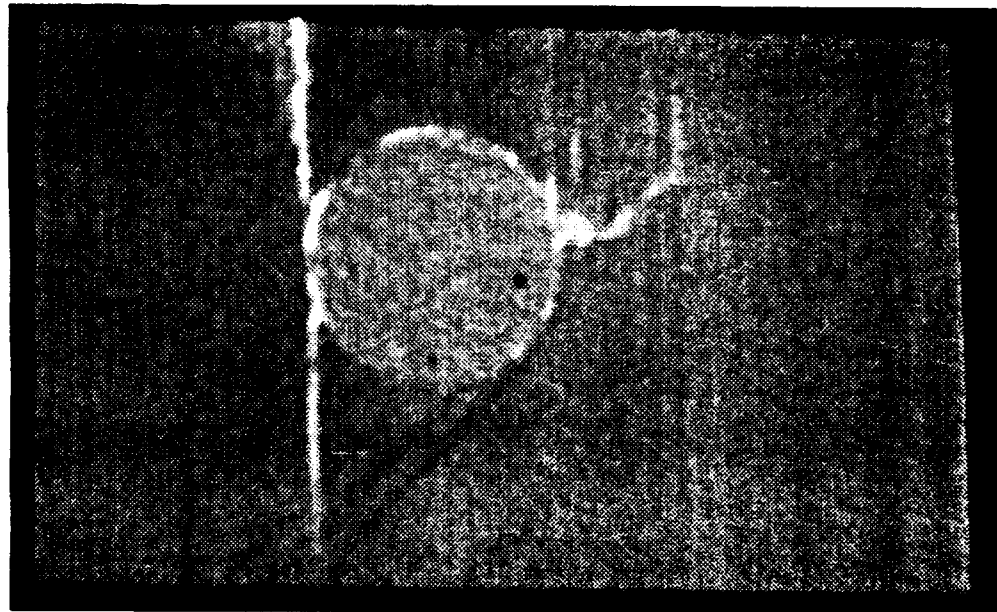


Figure 6.2-3 CT slice through a damaged graphite epoxy sample showing a transverse crack and a 0 degree crack intersecting a fastener hole.

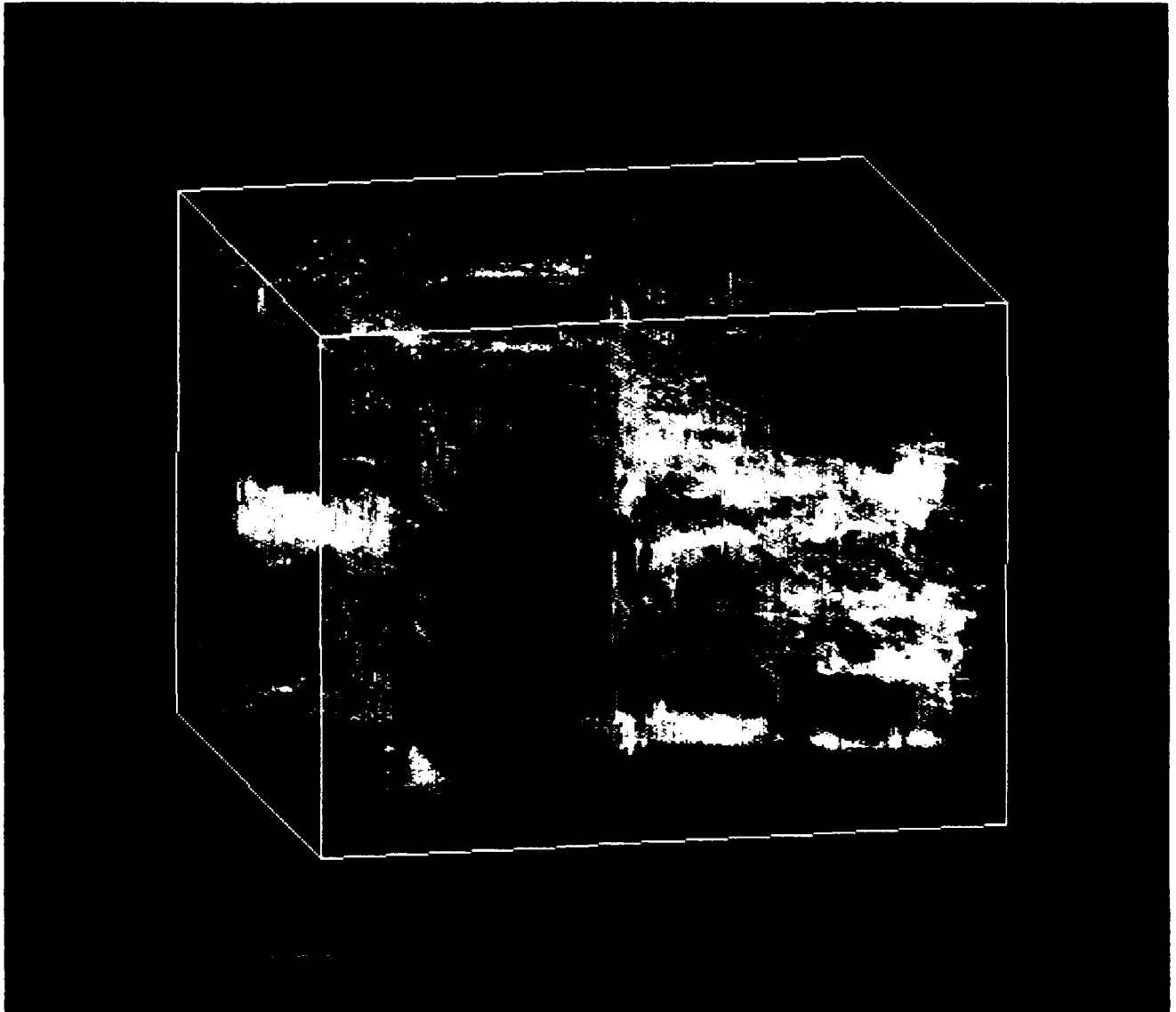


Figure 6.2-4 Three-dimensional model of the damaged region around a fastener hole constructed from high resolution CT data.

7.0 COST BENEFIT ANALYSIS

7.1 Failure Analysis Laboratory Application

A CT evaluation can have a significant impact on cost, confidence and time required to perform a failure analysis study, and will preserve the component in its original condition for disposition. Tables 7.1-1 and 7.1-2 are listings of the workload in 1 year (1990) for two aerospace failure analysis laboratories: a Parts Engineering Failure Analysis laboratory which generally handles electrical and electromechanical components, and an Equipment Quality Analysis laboratory which typically handles mechanical and electromechanical systems. Those items that would benefit from CT examination are noted in the tables. About 36 percent of the Parts Analysis laboratory workload and 10 percent of the Equipment Quality Analysis laboratory workload have been identified as having potential benefits from CT examination. The Parts Analysis laboratory in 1990 actually received an additional 45 components (about 18 percent of the total) that performed as designed and were not failed. Therefore, the 36 percent CT applicability criteria applies to the 82 percent of total components received that were analyzed for failure.

Table 7.1-1 Workload for Parts Engineering Failure Analysis Lab.

Category of Request	%	Total	O	B	D	C	NA
1990 Failure Tests	82%	205	2	40	31	5	127
Percent of Failures			1%	20%	15%	2%	62%
Electromechanical	36%	74	1	21	12	3	37
Electrical	58%	119	1	18	17	2	81
Mechanical	2%	5	-	-	2	-	3
Materials	3%	6	-	1	-	-	5
Unspecified	1%	1	-	-	-	-	1
O-Only B-Best D-Duplicate C-Too Costly NA-Not Applicable							

Table 7.1-2 Workload for Equipment Quality Analysis Lab.

Category of Request	%	Total	O	B	D	C	NA
1990 Total	100%	215	1	5	13	7	190
Percent of 1990 Total			1%	2%	6%	3%	88%
Electromechanical	26%	56	-	1	-	5	51
Electrical	15%	33	1	1	5	-	26
Mechanical	59%	126	-	3	8	2	113
Materials	%	-	-	-	-	-	-
Unspecified	%	-	-	-	-	-	-
O-Only B-Best D-Duplicate C-Too Costly NA-Not Applicable							

The evaluation categories used in the tables are "Only" (O), "Best" (B), "Duplicate" (D), "Too Costly" (C), and "Not Applicable" (N). The "Only" category is where there is no current inspection method that can provide the necessary information. The maximum financial benefit

for the "Only" category is where anomalous test results are encountered without an obvious failure. In this case, damage to the part looking for information should be avoided, yet technical integrity requires the understanding of reasons for the results so as to prevent the same thing happening again. This category is characterized by antenna and circuit boards from the Parts Failure Analysis laboratory and densitometers from the Equipment Quality Assurance laboratory.

The "Best" category is where the "act of observation" perturbs the system; this is fairly obvious in the case of destructive physical sectioning, but not so obvious in the case of disassembly where the stress and forces are released. The change in internal stress and force can lead to changes the failure/part configuration or destroy the evidence. The current culture is one of just expecting to destructively sample things because it is required. A close examination of the actual information required, without bias towards inspection technique, would reveal opportunities for savings in part and inspection costs. This category is characterized by relays from the Parts Failure Analysis laboratory and overheat detectors from the Equipment Quality Assurance laboratory.

The "Duplicate" category is where CT can provide the desired information about the part with the expense or time required being approximately the same as the traditional inspection method. The advantage of CT, however, is that it is nondestructive, retaining the component integrity should the result of the evaluation allow alternative disposition rather than destruction. The key to changeover to the use of CT would be based on acceptance of the CT data by analysts, availability, and ready access.

The "Not Cost Effective" category is where CT can provide the desired information about the part with the expense or time required being excessive compared to the traditional inspection method. In order for CT to become effective, it will require technology to advance such that overall scan time is reduced by an approximate factor of 10, with volume imaging and 3-D reconstruction required in many of these cases.

The "Not Applicable" category is where CT cannot provide the desired information about the part or the traditional inspection method is fully adequate and CT would be redundant.

The type of CT system will greatly affect the economics in terms of the cost of evaluation and type of components that can be examined. Table 7.1-3 categorizes several generic types of CT systems, including their rough approximate costs. These are general ranges for performance and specific systems may perform outside of the categories. Figure 7.1-1 shows graphically the relative performance of the systems types from Table 7.1-3 systems as a function of the part size and resolution ranges. Figure 7.1-2 is a bar graph showing the approximate percentage of components from the failure analysis laboratories of Tables 7.1-1 and 7.1-2 that would be applicable to the general types of CT systems.

The CT scanning time is a critical factor in evaluating the applicability of CT systems that has not been included in Table 7.1-3. Roughly, industrial CT systems typically operate with scan times of several minutes to tens of minutes depending on the test object size. For small components, such as in the electronics area, it is possible to have scan times as low as a 1-minute/slice depending on the CT system design. The use of cone beam CT (see Appendix Section A3.2) to obtain many CT slices for volume imaging in one scan period is another approach for increasing data acquisition speed that has considerable promise.

The Parts Failure Analysis laboratory would benefit most from a low cost microfocus based CT system with relatively rapid (approximately 1 minute or less) CT scanning capability. The Equipment Quality Analysis laboratory would require a more expensive CT system with the capability to handle large mechanical parts.

Table 7.1-3 Categories of CT Systems

Type	Source	Part Size	Resolution	Approx. Cost
A	Microfocus source	5 - 150 mm	0.025 - 0.25 mm	\$300K
B	Conventional tube	25 - 400 mm	0.2 - 0.5 mm	\$600K
C	Conventional tube	100 - 800 mm	0.4 - 0.75 mm	\$1 - 2M
D	Linacs	400 - 1800 mm	0.55 - 0.95 mm	\$2 - 3M

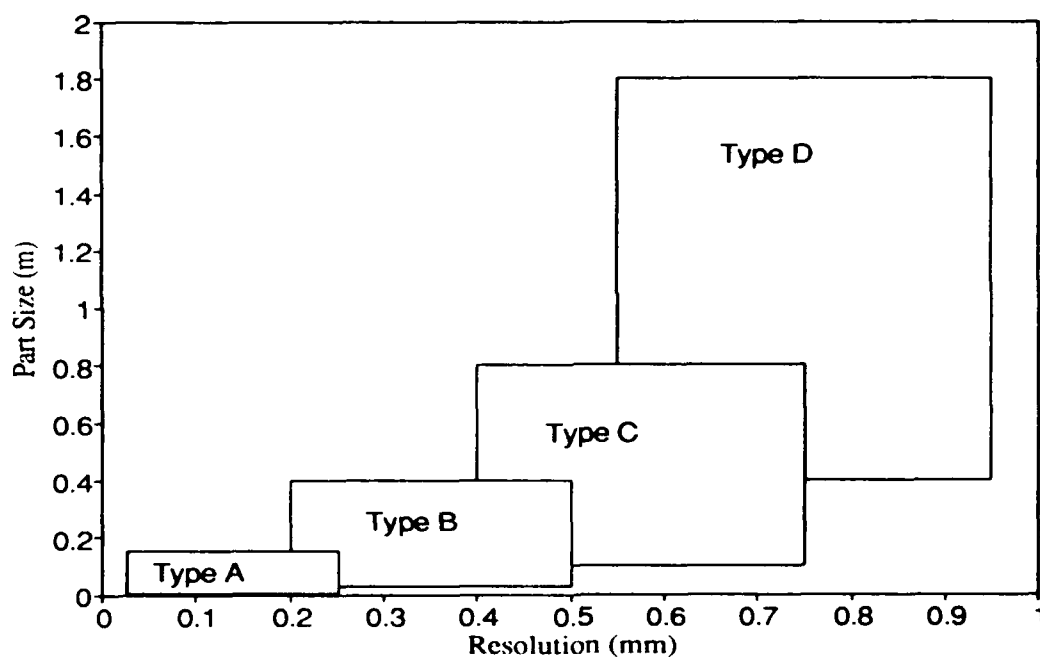


Figure 7.1-1 Approximate performance range for the CT systems of Table 7.1-3.

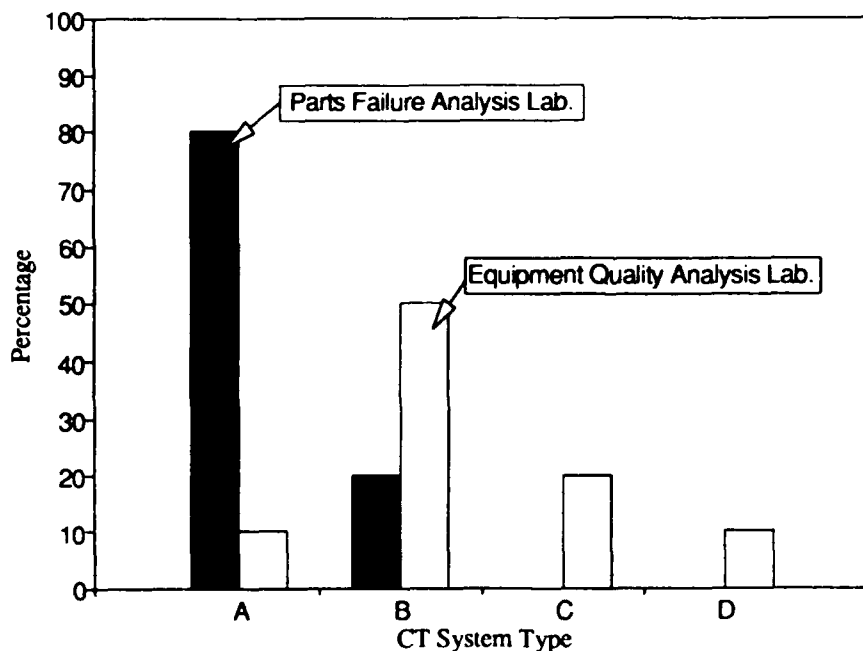


Figure 7.1-2 Bargraph showing the relative percentage of the workload applicable to each CT system type for the failure analysis laboratories.

7.2 Cost Savings Examples

7.2-1 Autobrake Modules

Verification of the faults in the autobrakes, without disassembly and breaking of the lead seals/lockwires, provided adequate evidence to the manufacturers without the need of convening an immediate failure analysis teardown. Such a teardown would require the presence of a number of key individuals. In the case of the unit with the displaced spring, it will be torn down in the future when the manufacturers' representatives are either here for other business or enough malfunctioning units have accumulated to justify the expense. The fact that it is clear that the spring is out of detent rather than possibly just dragging in the cavity will allow engineering to pursue causes and remedies for this problem. Normally these findings, without disassembly and breaking of the "seals," allow the airframe manufacturer to have the units repaired/replaced (\$3,000-\$4,000 unit cost) at the suppliers cost, under warranty.

7.2-2 Instrumentation Wafer Antenna

The wafer antenna has an approximate cost of \$13,000. The CT measurement provided the Go/No-Go information which should result in savings of at least one assembly for approximately \$13,000. The data and the information gained are being used in a process improvement effort to improve the product yield.

7.2-3 Raceway Potted Cable Assembly

The potted cable assemblies were valued at approximately \$30,000 per unit. The failure rate for faults which could be detected and/or evaluated by CT was approximately 50%. In the beginning of the production cycle, there would be significant improvements to the product development resulting from the CT evaluations, which would taper off with time as the product is refined. On a production run of 700 cables, the information gained should have been responsible for reducing the failure rate by 2% or 14 cables at \$30,000 each for \$420,000 total savings. This is projected savings since CT was used as a development tool and the program was cancelled before full-scale production.

7.3 CT System Procurement

The most likely area for CT system acquisition in failure analysis is the electronic, small electrical, and electromechanical device evaluation laboratories. Fundamentally this is because a CT system that will handle the small parts can be obtained for \$300K or possibly even less. Such laboratories use scanning electron microscopes routinely which themselves can cost between \$100K to \$300K, not unlike a small CT system. Using the extrapolation of experience from an aerospace parts analysis laboratory, the curves of Figure 7.3-1 have been generated.

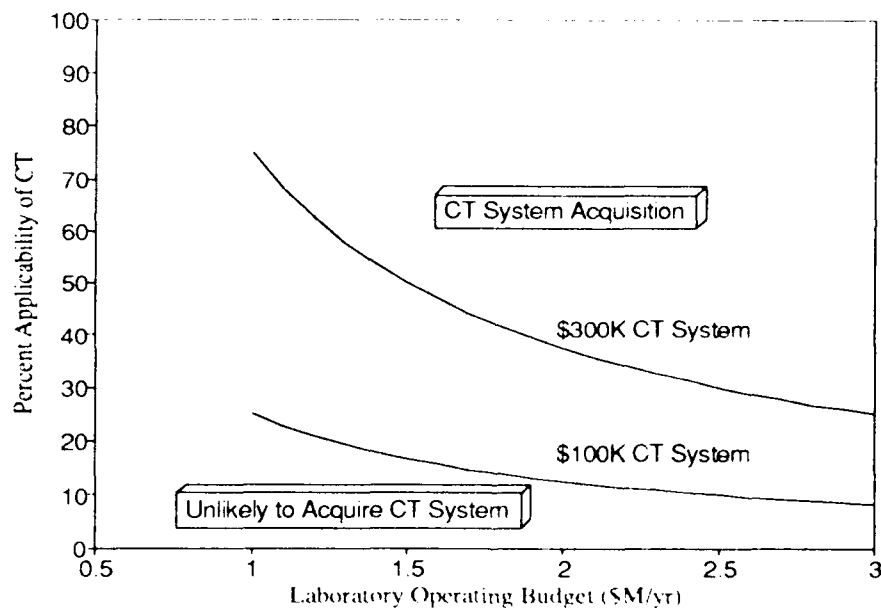


Figure 7.3-1 Laboratory size for microfocus CT system acquisition for various percentages of CT applicability to product evaluation.

Figure 7.3-1 indicates that for a \$300K CT system roughly, a laboratory would have to be in the \$3M/year of activity range to justify a system based on an approximately 25 percent applicability of CT. If a CT system could be obtained for \$100K, then a \$1M/yr laboratory (which is probably very typical of many aerospace establishments) would consider acquisition of a CT system. As the applicability of CT increases, the size of laboratory that would acquire a system decreases.

8.0 CONCLUSIONS AND RECOMMENDATIONS

8.1 Conclusions

The computed tomography cross-sectional image information provides useful three-dimensional spatial details on material conditions that can be used to assess internal configurations nondestructively for failure analysis investigations. CT is particularly advantageous on complex systems, composite failure studies and testing under operational or environmental conditions. CT, as a tool available to a failure analysis laboratory, can provide a benefit to approximately 10 to 30 percent of the workload with a considerable economic benefit.

The largest area for use of CT in failure analysis studies appears to be in the electronic/electromechanical area. Failure analysis studies in these areas require high resolution CT systems for relatively small (less than 50-mm-diameter) components. A reasonably large laboratory (>\$500K/year workload) could justify a microfocus based CT system for such studies. The use of CT in failure analysis of larger electromechanical and mechanical systems does not appear to offer enough incentive to justify the acquisition of a CT system for that sole purpose. CT can, however, be used effectively from a service facility. However, in many cases the ability to obtain the service must be fast and with minimal difficulties in transportation of the parts and information. Also to make CT truly valuable, analysts must become familiar with the results and data manipulation possibilities. Presently CT is relatively new and, therefore, is overlooked in its capability to provide cost-effective information. CT can also be applied with the component undergoing operational conditions (pressure, temperature, mechanical actuation, etc.) provided the appropriate conditions or environment can be generated at the CT facility.

CT for composite material failure analysis evaluations has been shown to be a useful tool. However, it is too early in the understanding of composite failures to be able to evaluate the general economic benefits of CT. Material failure analysis requires very high resolution imaging, which with CT, limits the size of the component that may be examined. In some cases macrographic information from CT on larger composites may be useful. CT system acquisition can not be justified for material failure analysis alone, but CT service can be purchased as a service for this purpose.

For electromechanical and mechanical systems, there appears to be a need for at least 0.25 mm resolution with energies in excess of 420 kV, the energy being driven by units of greater physical size than the Autobrake modules. For electrical parts there is a need for 3-D imaging of electronic parts for contamination, wire detachment and connectors. The resolution required is finer than 0.25 mm. The specific area where failure analysis is often in question is capacitors, where high Z and low Z materials located in very small feature geometry (0.1 mm resolution or better). For composite material failure analysis, very high resolution (better than 0.05 mm) is desired. Rapid scanning is needed for the 3-D studies of articles such as relays or composite damage.

Scanning speed is a critical parameter for any CT system data acquisition. The use of multiple slice CT for three-dimensional modeling was useful in the case of composite damage analysis. It can also be useful in other failure analysis evaluations as well. The development of "cone beam" or volume viewing CT systems (see Appendix, Section A3.2 that have adequate inherent resolution and contrast sensitivity will make an important advance in providing economic implementation of CT imaging. The failure analysis studies indicate that a general purpose CT system would need the speed of medical systems, the high resolution available in small volume industrial systems, and capability to go to high energy. These are conflicting criteria for the construction of any one CT system. Thus the availability of a variety of systems is desirable.

Additionally there is a need for analysis tools that allow expeditious data reduction. Often the answers found with a CT scan results in more investigation. Rapid, interactive data reduction would reduce the nonrecurring costs, such as travel and setup when additional investigation result from the data analysis.

8.2 Recommendations

CT examination should be considered as a tool to be used by failure analysis laboratories. CT setup and data evaluation must consider the goals of the failure analysis. Because CT can in many cases be performed with the component under environmental conditions, this should be pursued. Also in failure analysis studies, it is recommended that whenever possible a known component be scanned with the unknown to assist in the interpretation of features and details.

A CT system need not necessarily be purchased, but should be available. A CT service capability, set up to readily assist failure analysis organizations with scanning and interpretation could be worthwhile if a sufficient number of failure analysis laboratories would participate. In very large organizations, the failure analysis needs extend across many groups and they all need to be aware of the availability and applicability of CT to assist them in performing their functions better. For electronic failure analysis laboratories of sufficient size, a small microfocus based CT system would be a worthwhile acquisition. The system could provide multipurpose high resolution real-time or digital radiographic examinations as well. Such a system would be in the range of expense of scanning electron microscopes, which are common tools of these laboratories.

In general, educational material on the benefits of CT examinations need to be disseminated to failure analysis organizations. A demonstration to industry and government on how CT can be applied in a variety of failure analysis studies would be one method of education.

9.0 REFERENCES

1. R. H. Bossi, R. J. Kruse and B. W. Knutson, "Computed Tomography of Electronics", WRDC-TR-89-4112, December 1989.
2. R. H. Bossi, J. L. Cline and B. W. Knutson, "Computed Tomography of Thermal Batteries and Other Closed Systems," WRDC-TR-89-4113, December 1989.
3. R. H. Bossi, J. L. Cline, E. G. Costello and B. W. Knutson, "X-Ray Computed Tomography of Castings," WRDC-TR-89-4138, March 1990.
4. R. H. Bossi, K. K. Coopridge, and G. E. Georgeson, "X-Ray Computed Tomography of Composites" WRDC-TR-90-4014, July 1990.
5. P. Burstein and R. H. Bossi, "A Guide to Computed Tomography System Specifications" WRDC-TR-90-4026, August 1990.
6. R. H. Bossi and R. J. Kruse, "X-ray Tomographic Inspection of Printed Wiring Assemblies and Electrical Components," WRDC-TR-90-4091, October 1990.
7. G. E. Georgeson and R. H. Bossi, "X-Ray Computed Tomography of Full-Scale Castings," WL-TR-91-4049, October, 1991.
8. R. H. Bossi and G. E. Georgeson, "Computed Tomography Analysis of Castings," WL-TR-91-4121, January, 1992.
9. R. H. Bossi and J. L. Cline, "High Resolution X-Ray Computed Tomography," WL-TR-91-4102, (to be released).
10. J. M. Nelson, "Elevated Temperature Deformation Analysis," PL-TR-91-3019, June 1991.
11. R. Haralick, S. Sternberg and X. Zhuang, "Image Analysis Using Mathematical Morphology," IEEE Transactions on Pattern Analysis and Machine Intelligence, Vol. PAMI-9, No. 4, July 1987.

APPENDIX - RADIOGRAPHIC TECHNIQUES

The three techniques of radiographic imaging discussed in this report are film radiography, digital radiography, and computed tomography.

A1 Film Radiography

Conventional film radiography, as illustrated in Figure A1-1, uses a two-dimensional radiographic film to record the attenuation of the X-ray radiation passing through a three-dimensional object. This results in a shadowgraph containing the superposition of all of the object features in the image and often requires a skilled radiographer to interpret. The sensitivity in the image is determined by the attenuation coefficient for the material at the effective energy of the radiation beam, response of the X-ray film, film resolution, X-ray source spot size, and source-to-object-to-detector geometry. For electromechanical systems, which often vary in materials and thickness, the appropriate X-ray exposure will vary for different areas of the part and can only be compensated for by multiple exposures at different energies or times, and/or multiple views at a variety of orientations to the part.

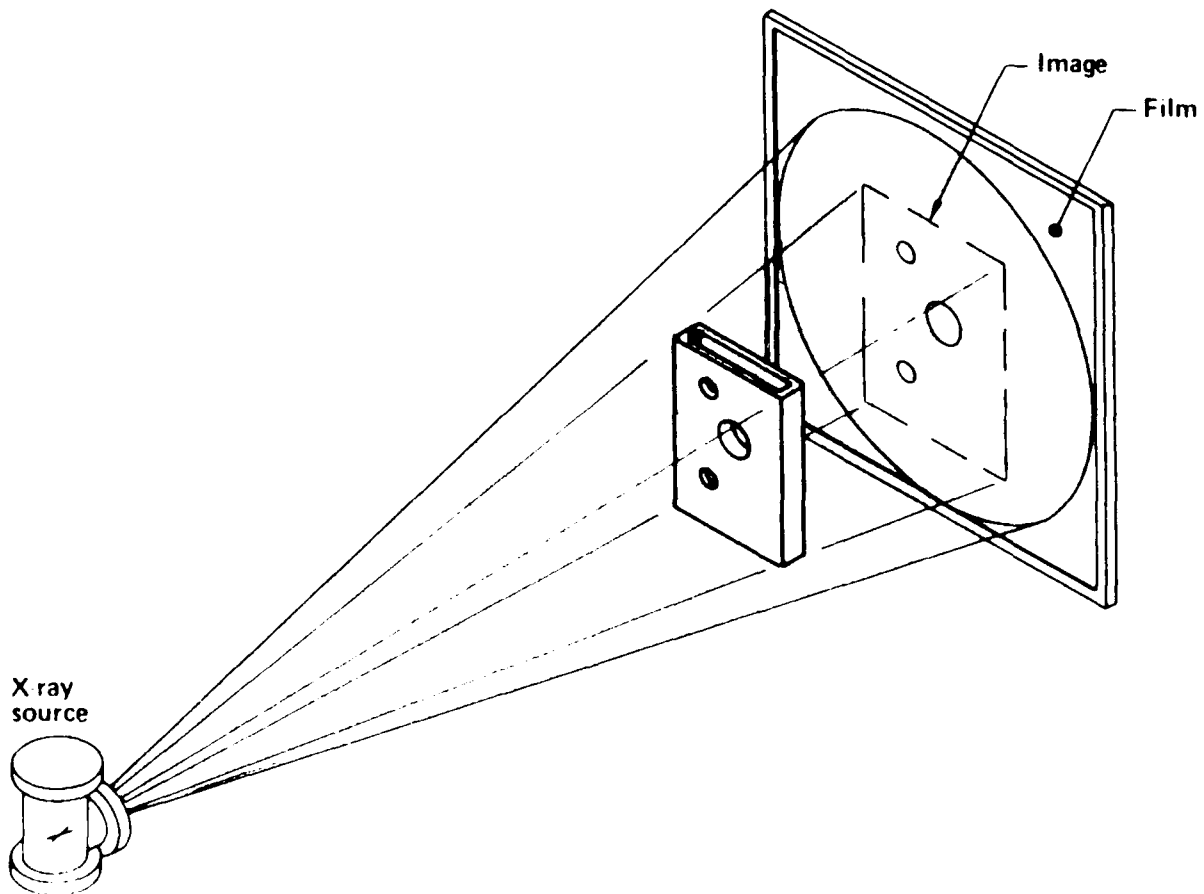


Figure A1-1 Film radiography.

Digital radiography (DR) is similar to conventional film radiography. The DR is performed on a system where the film is replaced by a linear array of detectors and the X-ray beam is collimated into a fan beam as shown in Figure A2-1. The object is moved perpendicular to the detector array, and the attenuated radiation is digitally sampled by the detectors. The data are 'stacked' up in a computer memory and displayed as an image. The sensitivity is determined by the geometric factors, and the resolution, signal-to-noise and dynamic range of the detector array. Usually DR images have a sufficiently large dynamic range that allows a wide range of the thickness or materials in a part to be imaged at suitable signal to noise with one scan.

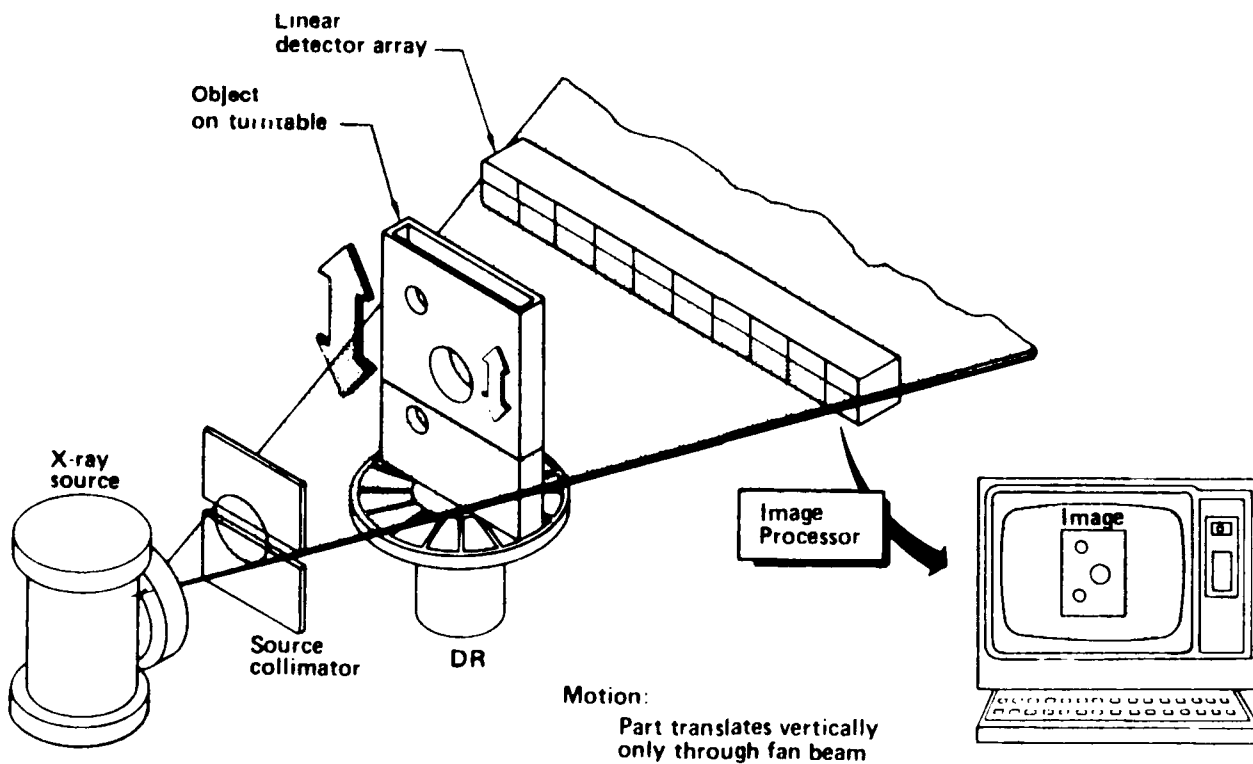


Figure A2-1 Digital radiography.

Computed tomography (CT) uses X-ray transmission information from numerous angles about an object to computer reconstruct cross sectional images (i.e., slices) of the interior structure. To generate a CT image, X-ray transmission is measured by an array of detectors. Data are obtained by translating and rotating the object so that many viewing angles about the object are used. A computer mathematically reconstructs the cross-sectional image from the multiple view data collected. A primary benefit of CT is that features are not superimposed in the image, thus making it easier to interpret than radiographic projection images. The image data points are small volumetric measurements directly related to the X-ray attenuation coefficient of the material present in the volume elements defined by the slice thickness and the horizontal resolution capability of the CT system. The values and locations provide quantitative data for dimensional and material density/constituent measurements.

A3.1 Conventional CT

Conventional CT is shown in Figure A3-1. The X-ray beam is collimated to a narrow slit and aligned with a detector array to define a CT slice plane in the component. For 100 percent coverage, multiple, contiguous slices must be taken over the entire component.

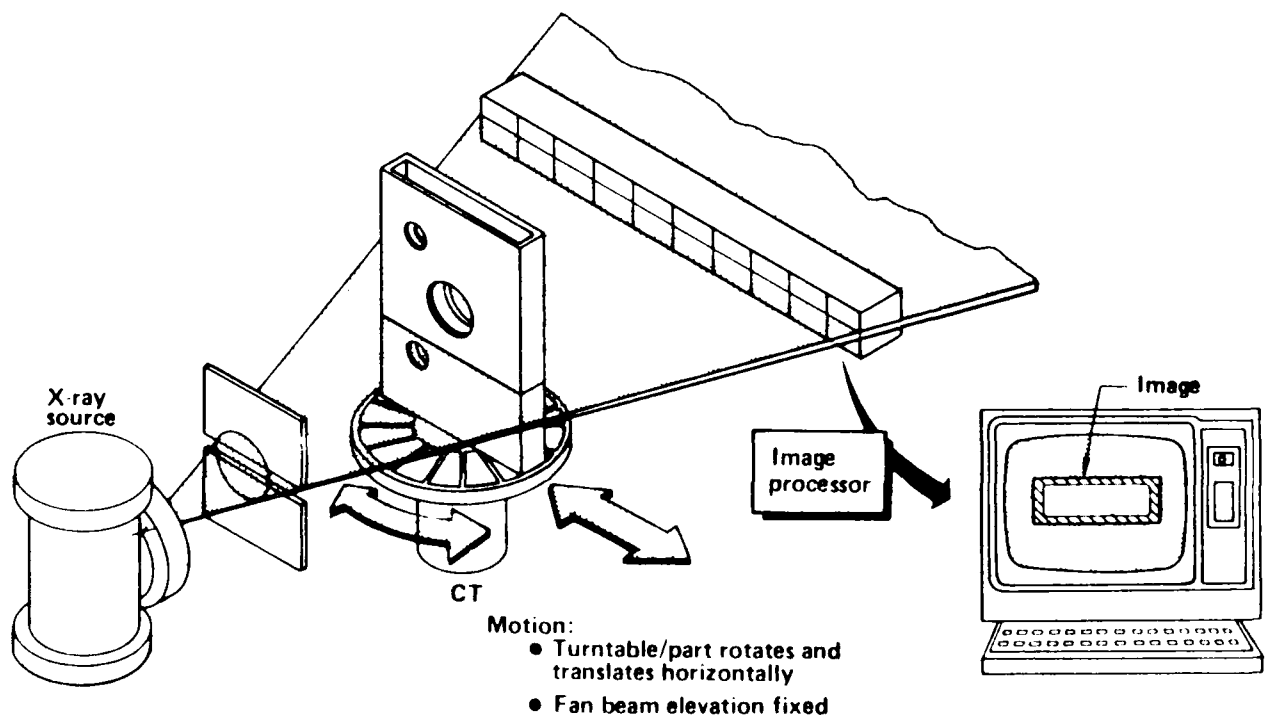


Figure A3-1 Computed tomography.

Cone beam CT is fundamentally the same as conventional CT; however, instead of collimating to a thin slice of radiation and using a linear detector array, an entire cone of radiation is used with an area array detector, as shown in Figure A3-2. The data acquisition in each angular view includes information for multiple CT slices along the object axis. The object will be rotated for data acquisition of multiple views. The data handling and reconstruction for cone beam CT is substantially more complicated than conventional CT, and a suitable display mechanism for viewing multiple plane images from the volumetric data set is needed. The advantage of the technique is that an entire volume can be scanned much more rapidly than is possible using conventional CT and taking scans at multiple axial positions. This offers a substantial cost savings for CT examinations of entire volumes.

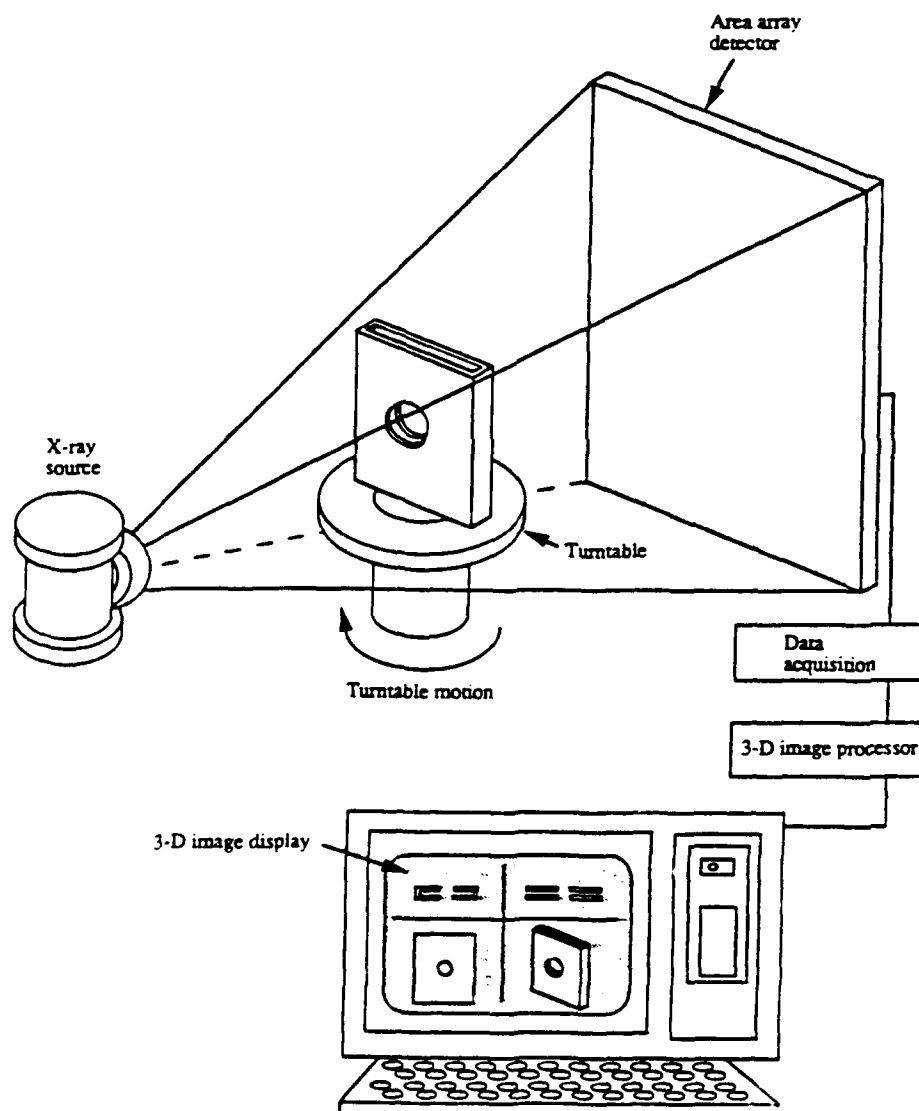


Figure A3-2 Cone beam CT.